

AN ABSTRACT OF THE THESIS OF

Daryl E. Hershberger for the degree of Master of Science  
in Nuclear Engineering presented on December 2, 1982

Title: Investigation of Special RETRAN Modeling Options  
with Regard to BWR Stability Under Natural Circulation  
Conditions. Redacted for Privacy

Abstract approved:

K. Hornyik

The limiting conditions of operation with regard to system stability for BWRs are presently set using computer models which employ conservative assumptions regarding the mechanisms which affect stability. Development of BWR models using "best estimate" codes, such as RETRAN, may allow more exact stability limits to be determined and precise stability margins to be set.

In this study, options regarding the specification of a time-dependent thermodynamic boundary condition as a method of introducing a perturbation function are examined, along with the effects of several RETRAN modeling options and systems parameters on the stability characteristics of the system being modeled. These parametric studies were performed modeling the system under natural circulation cooling conditions.

The desired pressure, and a default value of zero for the quality, were found to produce meaningful results when used to specify the time dependent conditions in the steam dome. The results were independent of the size of the time-dependent steam dome volume , so long as the flow length in the volume remained the same.

The results of the parametric studies showed that changes in the suction flow area used in the jet pump model have no effect on the stability of the system so long as the total core flow is unchanged. The homologous pump head curves were found to have a small effect on the system stability through their role in determining the total core flow. Comparison of the two-phase-flow models revealed that the homogeneous equilibrium mixture model produced less system stability than the algebraic slip model. The manner in which the RETRAN code calculates the reactivity feedback for the core volume in which the boiling boundary is located was found to produce a "nodal" effect which prevented any valid assessment of the effect of the axial power profile on the stability characteristics of the system. It was determined, however, that system stability is reduced when the reactor power level is increased.

**Investigation of Special RETRAN Modeling  
Options with Regard to BWR Stability  
Under Natural Circulation Conditions**

by

**Daryl E. Hershberger**

A THESIS

submitted to

**Oregon State University**

in partial fulfillment of  
the requirements for the  
degree of  
**Master of Science**

Commencement June 1983

APPROVED:

Redacted for Privacy

Professor of Nuclear Engineering in charge of major

Redacted for Privacy

Head of Department of Nuclear Engineering

Redacted for Privacy

Dean of Graduate School

Date thesis is presented 2 Dec. 1982

Typed by Daryl Hershberger

## ACKNOWLEDGEMENTS

I would especially like to thank my major professor, Dr. K. Hornyik, for the guidance and assistance given me on this project. His experience and insight into the phenomena encountered during this research were of invaluable aid to me.

A special thanks goes to Dr. B.I. Spinrad of O.S.U. and to the Institute of Nuclear Power Operation for providing me with the fellowship which financed my graduate education.

I would like to thank Dr. J. Naser and the Electrical Power Research Institute for providing computer facilities and access to the RETRAN code during this project.

Thanks also to Mr. S. Forkner of the Tennessee Valley Authority for providing a set of homologous pump curves.

Finally, thanks to my parents for the support they have given me throughout my graduate and undergraduate schooling.

## TABLE OF CONTENTS

	page
I. Introduction .....	1
II. The Simplified RETRAN Model .....	6
II.1. Simplified Model Description .....	6
II.2. Use of the Time Dependent Volume ....	10
II.2.1. Perturbation Signal .....	10
II.2.2. Specification of Time Dependent Conditions .....	17
II.2.3. "Infinite" Volume Model ....	23
II.3. Comparision of Simplified and Comprehensive Models .....	28
III. Parametric Studies Performed Under Natural Circulation Conditions .....	36
III.1. Determination of Steady State Natural Circulation .....	36
III.1.1. Flow Boundary Conditions ....	37
III.1.2. Internal Flow Conditions ....	38
III.2. Recirculation System Model .....	40
III.2.1. Jet Pump Geometry .....	40
III.2.2. Homologous Pump Head Curves ..	46
III.3. Two-Phase-Flow Models .....	52
III.4. Natural Circulation at Full Power ..	59
III.4.1. Determining the Steady State .....	59
III.4.2. Axial Power Profile/ Nodal Effect .....	60
III.4.3. Stability at Full Power ....	63
IV. Conclusions .....	69

V. References ..... 71

VI. Appendix ..... 73

## LIST OF FIGURES

Figure	Page
1. Schematic diagram of RETRAN BWR model used for stability analysis (comprehensive model). . . . .	8
2. Schematic diagram of RETRAN BWR model used for stability analysis (simplified model). . . . .	9
3. Comparison of 48 point and 64 point representations of measured PB2 pressure transient. . . . .	14
4. Gain of pressure-to-flux transfer function obtained from simplified RETRAN model using 48 point and 64 point representations of pressure transient. . . . .	15
5. Phase shift of pressure-to-flux transfer function obtained from simplified RETRAN model using 48 point and 64 point representations of pressure transient. . . . .	16
6. Gain of pressure-to-flux transfer function obtained from simplified RETRAN model using constant steam dome qualities of 0.99998 and 0.0. . . . .	21
7. Phase shift of pressure-to-flux transfer function obtained from simplified RETRAN model using constant steam dome qualities of 0.99998 and 0.0. . . . .	22
8. Gain of pressure-to-flux transfer function obtained from simplified RETRAN model using various steam dome dimensions. . . . .	26
9. Phase shift of pressure-to-flux transfer function obtained from simplified RETRAN model using various steam dome dimensions. . . . .	27
10. Steam dome pressure transients obtained from the comprehensive RETRAN model and by Fourier synthesis. . . . .	32

Figure		Page
11.	Calculated power transients obtained from comprehensive and simplified RETRAN models. ....	33
12.	Gain of pressure-to-flux transfer function obtained from comprehensive and simplified RETRAN models. ....	34
13.	Phase shift of pressure-to-flux transfer function obtained from comprehensive and simplified RETRAN models. ....	35
14.	Schematic diagram of RETRAN jet pump geometry. ....	43
15.	Gain of pressure-to-flux transfer function obtained from simplified RETRAN model for various values of the jet pump suction flow area. ....	44
16.	Phase shift of pressure-to-flux transfer function obtained from simplified RETRAN model for various values of the jet pump sution flow area. ....	45
17.	Homologous pump head curves used in simplified RETRAN model. ....	49
18.	Gain of pressure-to-flux transfer function obtained from simplified RETRAN model using various extrapolations of homologous pump head curves. ....	50
19.	Phase shift of pressure-to-flux transfer function obtained from simplified RETRAN model using various extrapolations of homologous pump head curves. ....	51
20.	Reactor power transients for HEM and ASM for two-phase-flow. ....	55
21.	Axial distribution of coolant void at steady state for HEM and ASM for two-phase-flow. ....	56
22.	Density transients for HEM and ASM for two-phase-flow. ....	57

Figure	Page
23. Reactor power transient limit cycle calculated using HEM for two-phase-flow. ....	58
24. RETRAN control volume/junction geometry. ....	64
25. Various axial power profiles used for 100% power cases. ....	65
26. Reactor power transients resulting from extreme cases of the "nodal" effect (ASM for two-phase-flow). ....	66
27. Reactor power transients resulting from extreme cases of the "nodal" effect (HEM for two-phase-flow). ....	67
28. Reactor power transients for 58.45% and 100% initial power. ....	68

## LIST OF TABLES

Table		page
1.	Input requirements for RETRAN time dependent volume. ....	20
2.	Initial junction #10 stagnation pressure differential, initial quality in volume #5, and decay ratios for various values of steam dome quality and axial power profiles. ....	20
3.	Steam dome geometry and decay ratios for finite and "infinite" volume models. ...	25
4.	Process parameters used to adjust unspecified loss coefficients. ....	39
5.	Flow rates and decay ratios obtained for various extrapolations of the RETRAN homologous pump head curves. ....	48

Investigation of Special RETRAN Modeling  
Options with Regard to BWR Stability  
Under Natural Circulation Conditions

I. INTRODUCTION

Under certain conditions of operation, i.e. low flow/power ratio, boiling water reactors (BWRs) are susceptible to instabilities in the form of reactor power-core flow oscillations. The mechanism behind these oscillations is the strong coupling which exists between reactor power and heat transfer to the coolant on the one side, and the effect of coolant density on neutron multiplication on the other<sup>1</sup>. At the present time these instabilities are prevented by limiting the combinations of reactor power and core flow at which BWRs are allowed to operate. These operational limits are based on analyses done with generic models of BWRs and using conservative assumptions concerning the mechanisms and parameters which affect stability. For this reason, the operational limits placed on BWRs do not represent the actual stability limits, but rather incorporate safety margins of uncertain magnitude. The development of more realistic "best estimate" models of BWRs will allow more accurate operational limits to be determined and may enable BWRs to operate at lower flow/power ratios than currently permitted. Operation under these conditions is desirable from the point of view of neutron economy.

A series of stability tests were performed at the Peach Bottom Atomic Power Station, Unit 2 (PB2), at the end of cycle 2 and during cycle 3, to provide benchmark data against which computer models of BWRs may be compared<sup>2</sup>. One such model, using the RETRAN code, was developed by Hornyik and Naser<sup>3</sup> to simulate the PB2 turbine trip tests and is being used by the same authors in a simulation of the PB2 stability tests.

The RETRAN (RELAP4 TRANSIENT) computer code was developed from the RELAP series of computer codes to describe the transient thermal-hydraulic behavior of light-water reactors. It is designed to provide "best estimate" solutions to accident and operational transient problems. A complete description of the RETRAN code can be found in EPRI report NP-1850, "RETRAN-02: A Program for One-Dimensional Transient Thermal-Hydraulic Analysis of Complex Fluid Flow Systems" volumes 1 thru 4.

The objective of this thesis is to verify a simplified version of this RETRAN model of PB2 and to use this simplified model to study the effects of various modeling options and input parameters on the calculated transient results and stability characteristics. Included in these objectives is the demonstration that the RETRAN model responds virtually

as a linear system when small perturbations are used.

In the simplified model the perturbation signal is introduced by specifying the condition in the steam dome as a function of time. This method replaces switching the pressure set point of the pressure regulator which was used in the actual plant test as well as in the comprehensive model. The basic assumption underlying this simplification is that the steam lines and pressure regulator do not affect those stability characteristics of the system which are of concern here.

The motivation for developing a simplified version of the RETRAN model is twofold. First, by reducing the extent to which the nuclear steam supply system (NSSS) is modeled, a reduction in computing time, and thus cost, is realized. Second, the removal of the steam lines, pressure regulator, etc. eliminates the uncertainties associated with those elements of the model.

The report is divided into two main parts: the description and use of the simplified model, and a study of natural circulation cooling conditions using the simplified RETRAN model.

A description of the simplified model, including a

discussion of options regarding the time dependent volume, and verification of the model, along with a comparison of results from the simplified and comprehensive models are presented in chapter 2.

In chapter 3 several system parameters and modeling options are examined in order to determine their effect on the calculated transient results while modeling natural circulation cooling conditions. They are:

- Jet pump modeling technique
- Homologous pump head curves
- Two-phase-flow models
- Axial power profile
- Reactor power level

These studies were performed using natural circulation cooling as experience indicates that BWRs have the least margin with respect to stability under these conditions.<sup>4</sup>

Time limitation prevented similar studies of other areas which are thought to be important, such as 1-D kinetics and the dynamic slip model.

The results of the computed system transient response for each case are expressed, for comparison, in the time domain and the frequency domain. The frequency domain analysis is based on the assumption that the RETRAN model behaves as a linear system, and consists of calculation of a steam dome pressure-to-neutron flux transfer function and of a decay ratio based on this transfer function. The use of the pressure-to-flux transfer function to describe the stability properties of the system derives from a novel feature of the PB2 stability tests. The tests were designed, in part, to show that small pressure perturbation tests could be used as an alternative to control rod oscillation tests in determining the stability margin with respect to neutron flux-void reactivity feedback in BWRs. The method used to calculate the pressure-to-flux transfer function from the output of the RETRAN model and a brief discussion of the decay ratio are given in the appendix of this thesis.

## II. THE SIMPLIFIED RETRAN MODEL

### II.1. Simplified Model Description

The RETRAN model which is used in these studies is a reduced or simplified version of a model which was developed for the simulation of the PB2 turbine trip tests and later modified slightly for study of the PB2 stability tests. The original model is described in detail in EPRI special report NP-1076-SR. Figures #1 and #2 show schematic drawings of the comprehensive and simplified models, respectively. In order to solve a transient problem with the RETRAN code, the system being modeled must be divided into a discrete number of control volumes. These volumes are connected to one another by flow paths or "junctions". The numbers which appear on the schematic of the simplified model are the identifying number associated with each volume described in the RETRAN code.

In the simplified model the steam lines, turbine, condenser, pressure regulator, and valves and the associated control system have been removed. What remains is the portion of the NSSS inside the pressure vessel and the recirculation lines and pumps. The thermodynamic properties of the coolant in the steam dome, volume #10, are specified as a function of time,

thus providing the perturbation of the system from its initial equilibrium state.

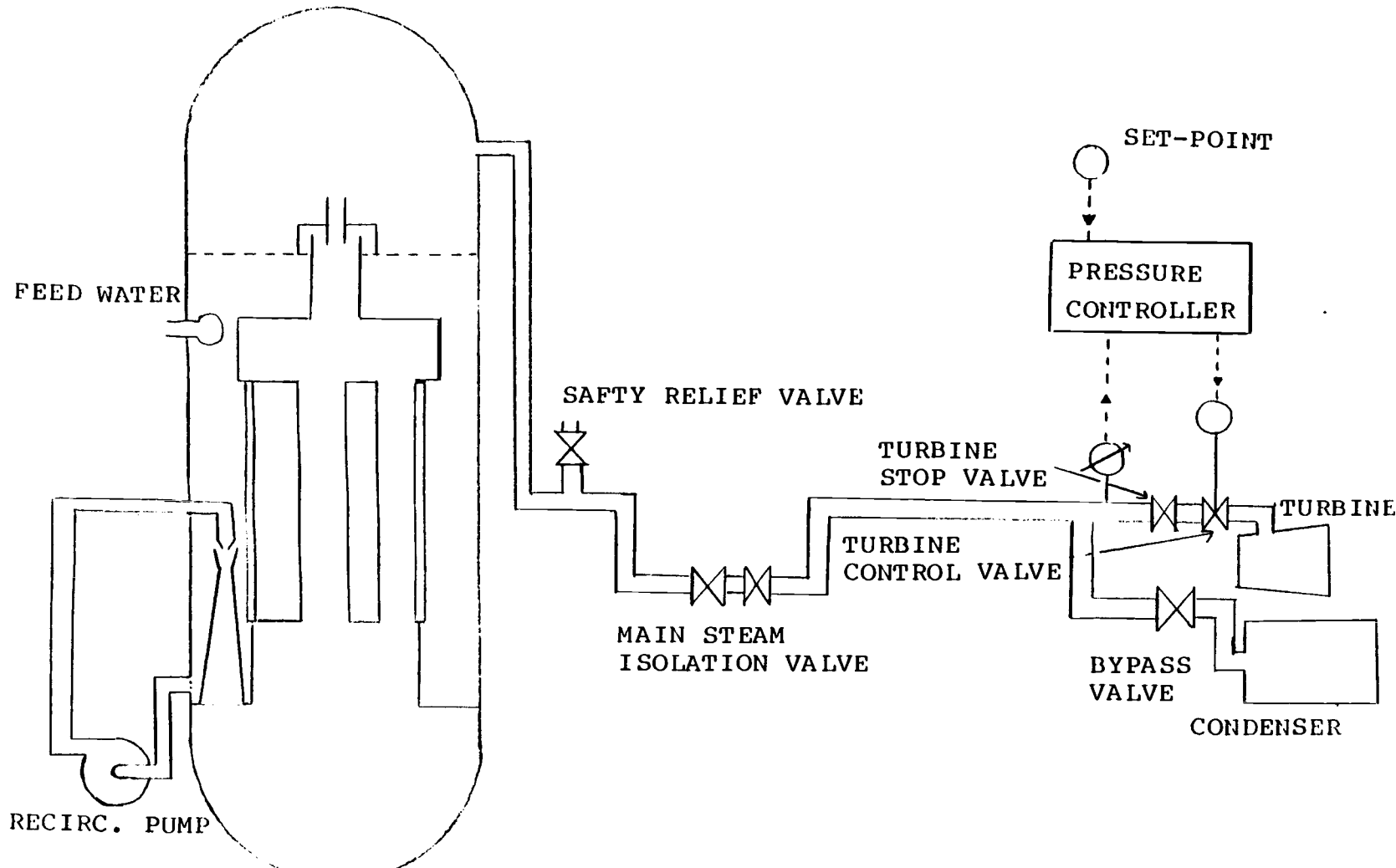


Figure 1. Schematic diagram of RETRAN BWR model used for stability analysis (comprehensive model).

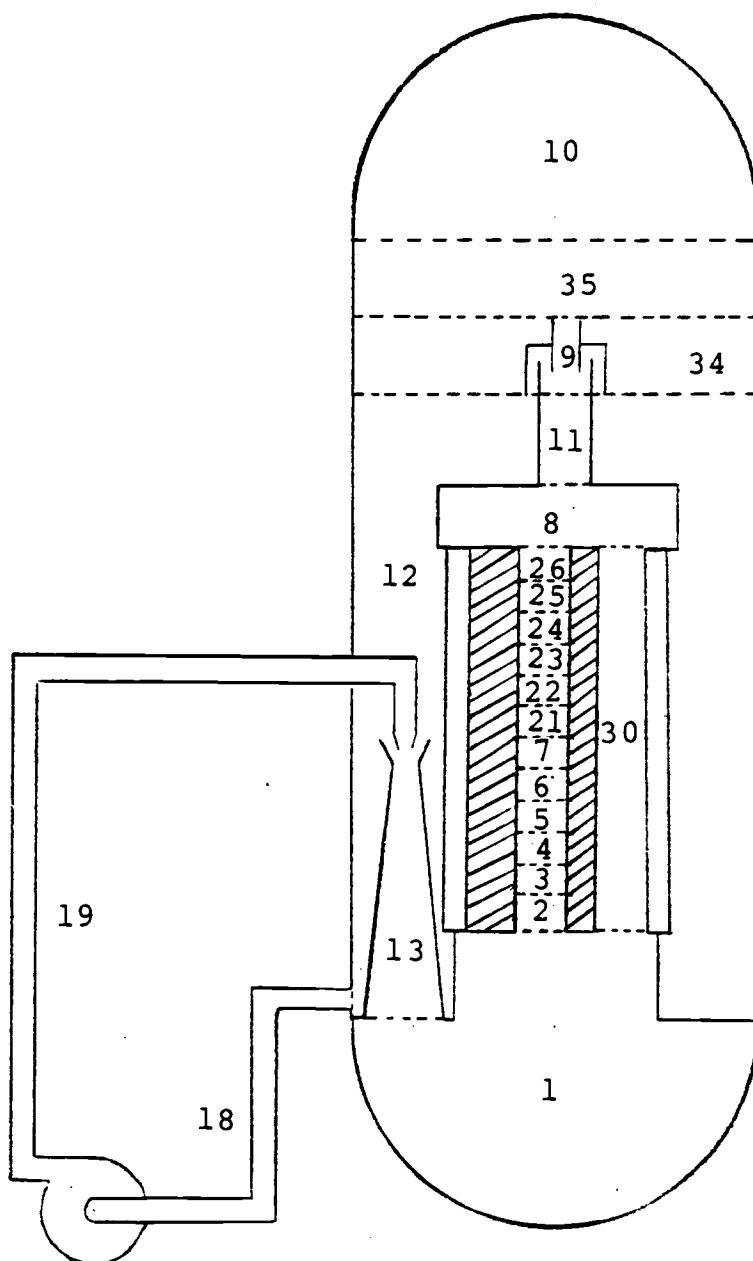


Figure 2: Schematic diagram of RETRAN BWR model used for stability analysis (simplified model).

## II.2. Use of the Time Dependent Volume

In the comprehensive model the perturbation is introduced by switching the pressure set point at periodic intervals as was done in the actual plant tests. With the removal of the pressure regulator an alternate method of introducing the perturbation must be used. In the simplified model the steam dome, volume #10, is designated a time dependent volume and the perturbation signal is input as a boundary condition by specifying the conditions in the steam dome as a function of time. Care must be taken in the specification of conditions in the time dependent volume, as they are discrete representations of a continuous function. Before the simplified model could be compared with the comprehensive model, a suitable perturbation signal and a set of thermodynamic variables for specifying the time dependent conditions had to be determined.

### II.2.1. Perturbation Signal

The object of the frequency domain analysis is the calculation of the steam dome pressure-to-neutron flux transfer function, and from this, a decay ratio. Because of the method used for the frequency domain analysis,

some constraints must be placed on the perturbation signal.

The frequency domain analysis is based on the assumption that the model behaves as a linear system. If the RETRAN Model were a linear model then the same transfer function would be obtained for any perturbation signal used. The RETRAN model is not, however, a linear model, but if the perturbation is small enough, the non-linearities will not show up<sup>5</sup>. One of the constraints then, on the perturbation signal, is that it must be small enough to produce a quasi-linear system response.

Another important constraint on the perturbation signal has to do with its frequency makeup. To remain consistent with the PB2 tests, a periodic signal with a 20 second period was used for this model. This translates to a minimum frequency component in the perturbation signal of 0.05 cps with the maximum frequency component present being determined by the number of data points used to represent the signal over one cycle<sup>6</sup>. The even-harmonic frequencies were not used in the PB2 tests because they were absent in the skew-symmetric perturbation function used. It is important that each of the odd-harmonic frequencies in the desired range be well represented in the

perturbation signal in order for the transfer function to retain its significance for that frequency range. A general limitation at the high frequency end of the spectrum was noted for this approach. This limit is attributed to discontinuities in some of the RETRAN models which themselves cause perturbations in the high frequency range (>1 cps).

Cases D14 and D15, which were the first attempts to use the measured PB2 steam dome pressure signal, illustrate the importance of the individual frequency makeup of the signal as opposed to just the overall shape of the signal. Figure #3 shows the steam dome pressure transients used for both cases. The pressure transient plots look almost identical, but in case D14 the curve is represented discretely by 48 points spaced unevenly over the 20 seconds while in case D15 the signal is represented by 64 points spaced at equal time intervals. The resulting transfer functions for both cases, plotted in figures #4 and #5, show differences in both the gain and phase shifts, especially in the higher frequencies.

Examination of the two representations of the perturbation function showed that while they appear to be the same in the time domain, their frequency make up is different. In the 48 point representation the

components of higher frequencies, where there is so much difference in the transfer functions, are substantially less than those of the 64 point case. This leads to the variations in the particular transfer function in the range of higher frequencies and thus provides a measure of the lack of resolution of the RETRAN model in this range. This lack of resolution is probably caused by numerical effects.

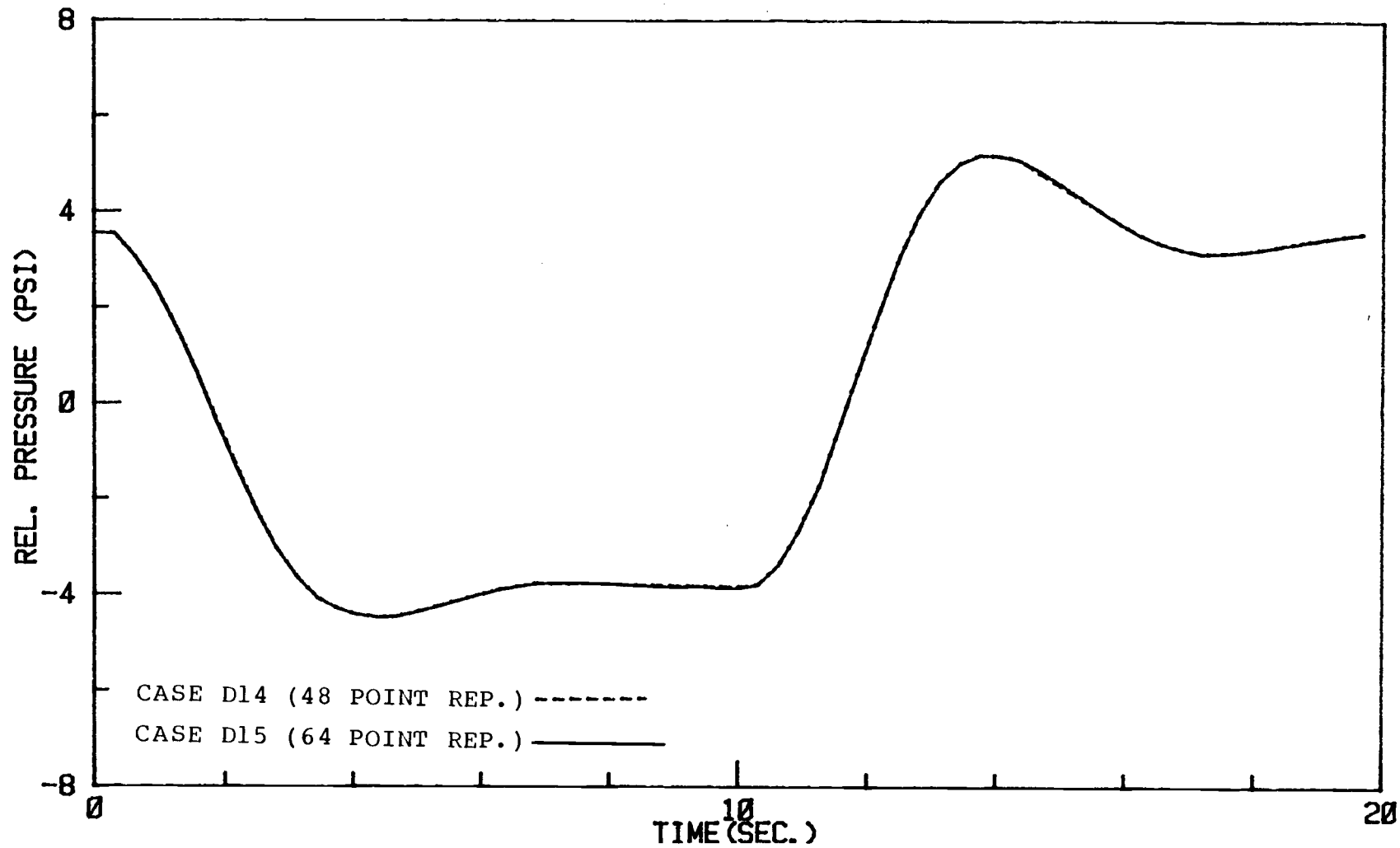


Figure 3. Comparison of 48 point and 64 point representations of measured PB2 pressure transient.

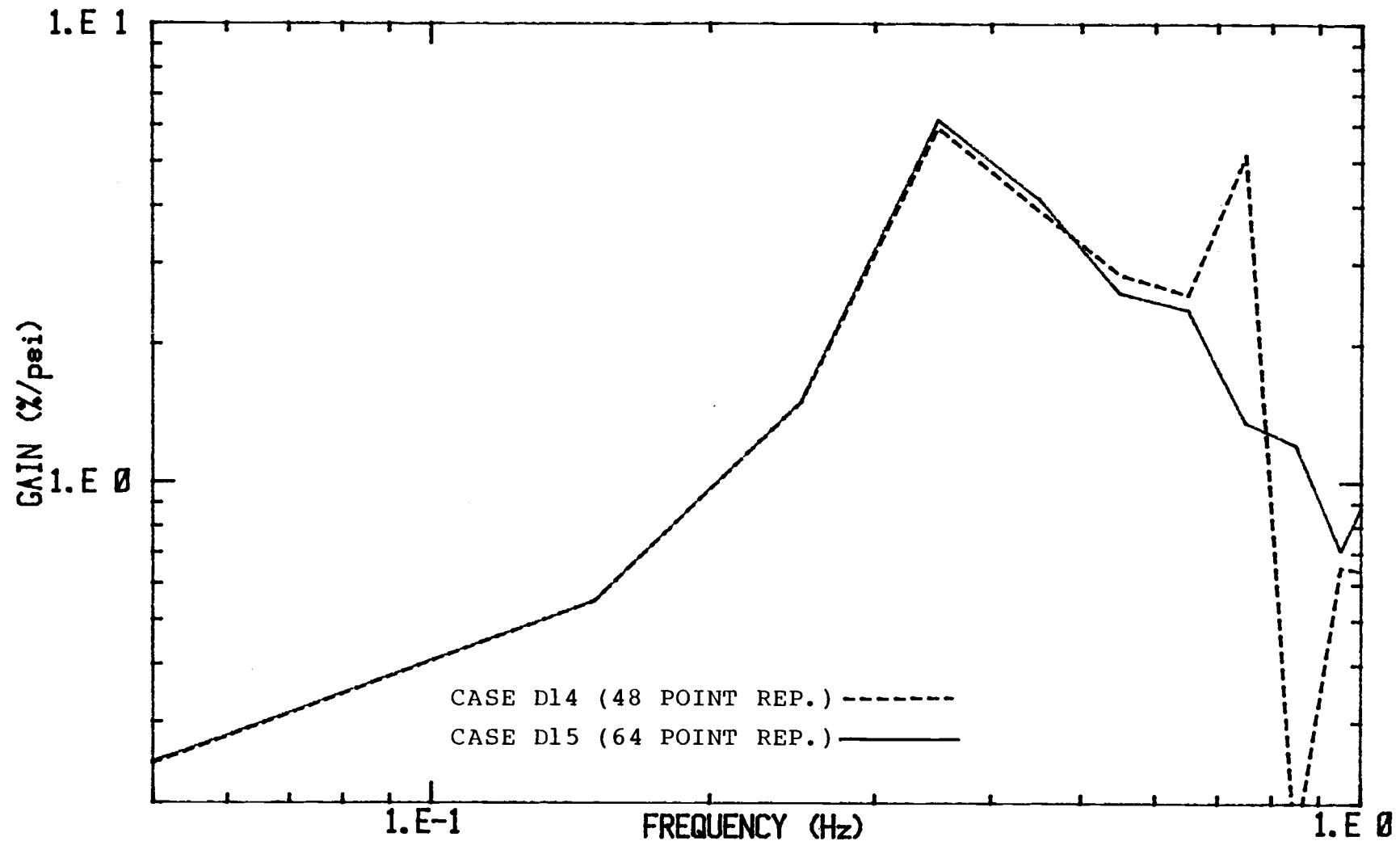


Figure 4. Gain of pressure-to-flux transfer function obtained from simplified RETRAN model using 48 point and 64 point representations of pressure transient.

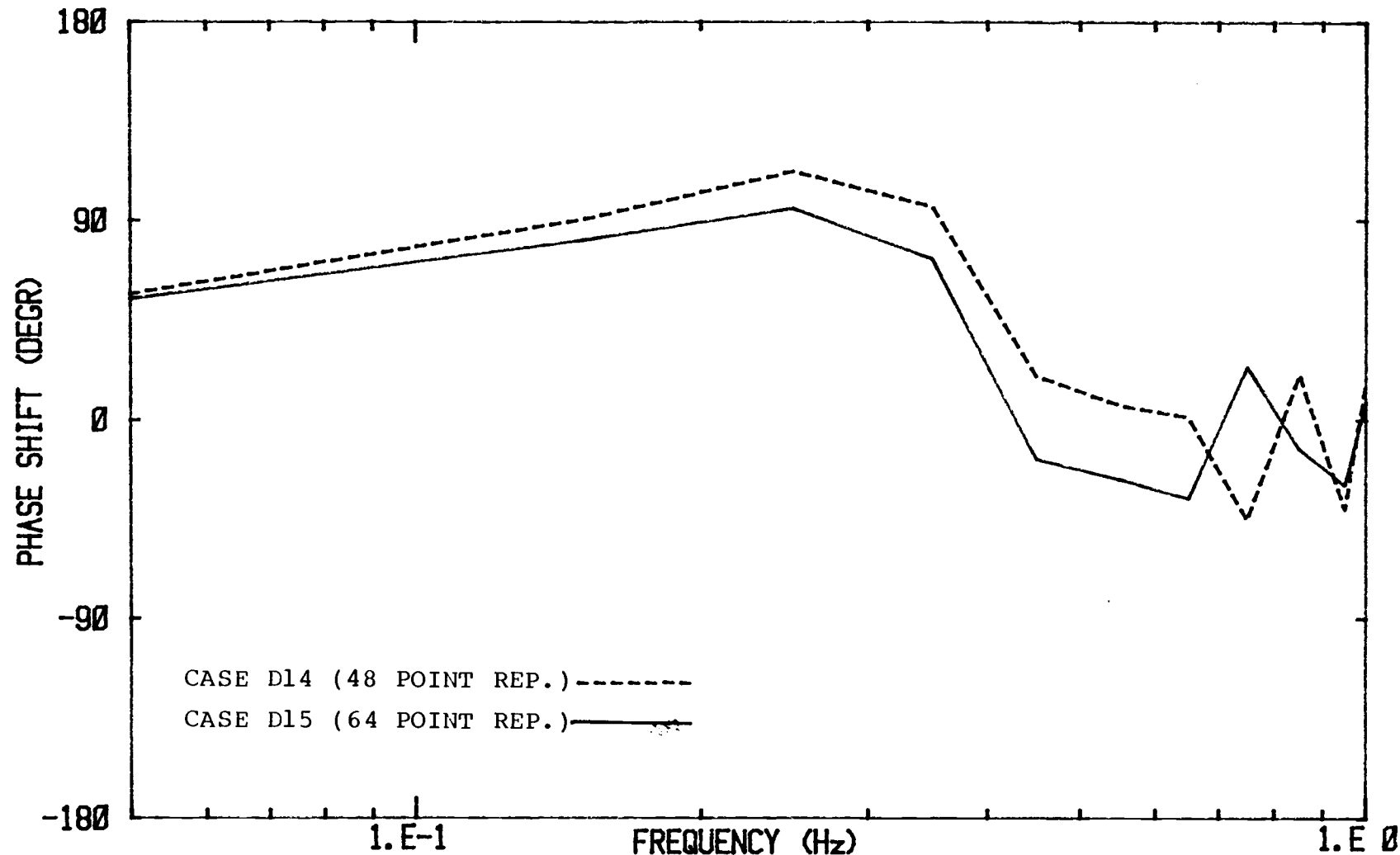


Figure 5. Phase shift of pressure-to-flux transfer function obtained from simplified RETRAN model using 48 point and 64 point representations of pressure transient.

### II.2.2. Specification of Time Dependent Conditions

In order to uniquely specify the conditions which exist in a RETRAN control volume, two independent thermodynamic variables must be given. Table #1 lists the combinations of pressure, temperature, and quality which may be used to specify the conditions in a RETRAN time-dependent volume<sup>7</sup>.

Various combinations of input specification for the steam dome were tried, as there was some lack of clarity in the input description for the code. An option found to produce meaningful results consisted of specifying the steam dome pressure along with a default value of zero for the quality. Pressure was chosen because it is the input variable of the transfer function of interest; also, it was the only one of the three thermodynamic variables which was measured directly during the PB2 tests. Although the actual quality of the coolant in the steam dome can be expected to be near 1.0, the method employing the default value was retained after it was found that the results of a particular transient calculation depended very little on the quality specified. A comparison of cases D21, D22, and D50 demonstrates the effect of the steam dome quality on the results for similar cases. Table #2 lists several important system parameters, as well as the decay ratio

for each of the three cases.

Cases D21 and D22 were identical, except for the quality which was used in specifying the conditions in the time dependent volume. A comparison of the transfer functions for these two cases, figure #6 and #7, shows a small difference in both the gain and phase shift, especially for frequencies above .40 Hz. The quality specified in the steam dome affects the rest of the system through the stagnation pressure differential associated with the junction connecting the steam dryer volume to the steam dome. The stagnation pressure differential across this junction plays a role in determining the pressures in the rest of the system, and through them the quality and void distribution in the core. The quality in volume #5, where the boiling boundary occurs, was found to have an important affect on the calculated transient results. This phenomenon is covered in section III.4.3.. Case D50 is a rerun of case D22 with the axial power profile altered slightly to provide the same initial quality in volume #5 as in case D21. The transfer function for case D50, also shown in figures #6 and #7, is much closer to that of case D21. Most of the remaining discrepancies can by attributed directly to the increase in stagnation pressure across the junction caused by the difference in steam dome quality and/or the change in the axial power profile.

As a result of this comparison, a constant quality of 0.0 and the desired pressure are used to specify the time dependent conditions in the steam dome.

Conditions Present	Thermodynamic Variables Used
Superheated Vapor	Pressure, Temperature *
Saturated Vapor	Temperature, Quality
Saturated Liquid	Temperature, Quality
Subcooled Liquid	Pressure, Temperature
Two-Phase-Mixture	Temperature, Quality

Table 1. Input requirements for RETRAN time dependent volumes.

CASE	D21	D22	D50
Vol.#10			
Quality	0.99998	0.0	0.0
Axial power profile	A	A	B
Stagnation pressure(psi)	1.5484E-1	2.41247	2.41247
Vol.#5			
Quality	1.344E-3	8.893E-4	1.336E-3
Decay Ratio	0.46676	0.49583	0.48018

Table 2. Initial junction #10 stagnation pressure differential, initial quality in volume #5, and decay ratios for various values of steam dome quality and axial power profiles.

\* The combination of variables used in this study, pressure and the default value for quality, is not listed in the input description of the code.

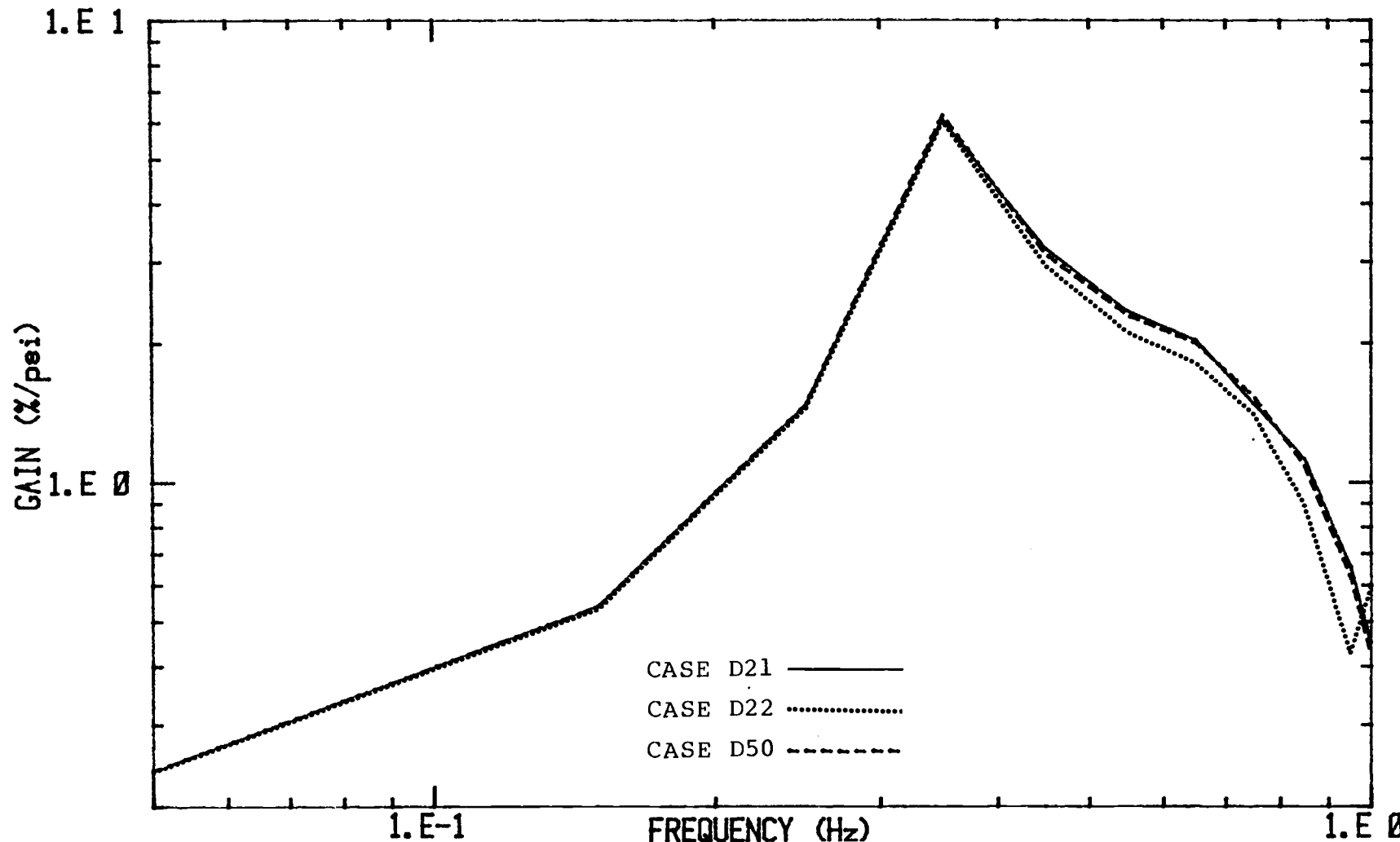


Figure 6. Gain of pressure-to-flux transfer function obtained from simplified RETRAN model using constant steam dome qualities of 0.99998 and 0.0.

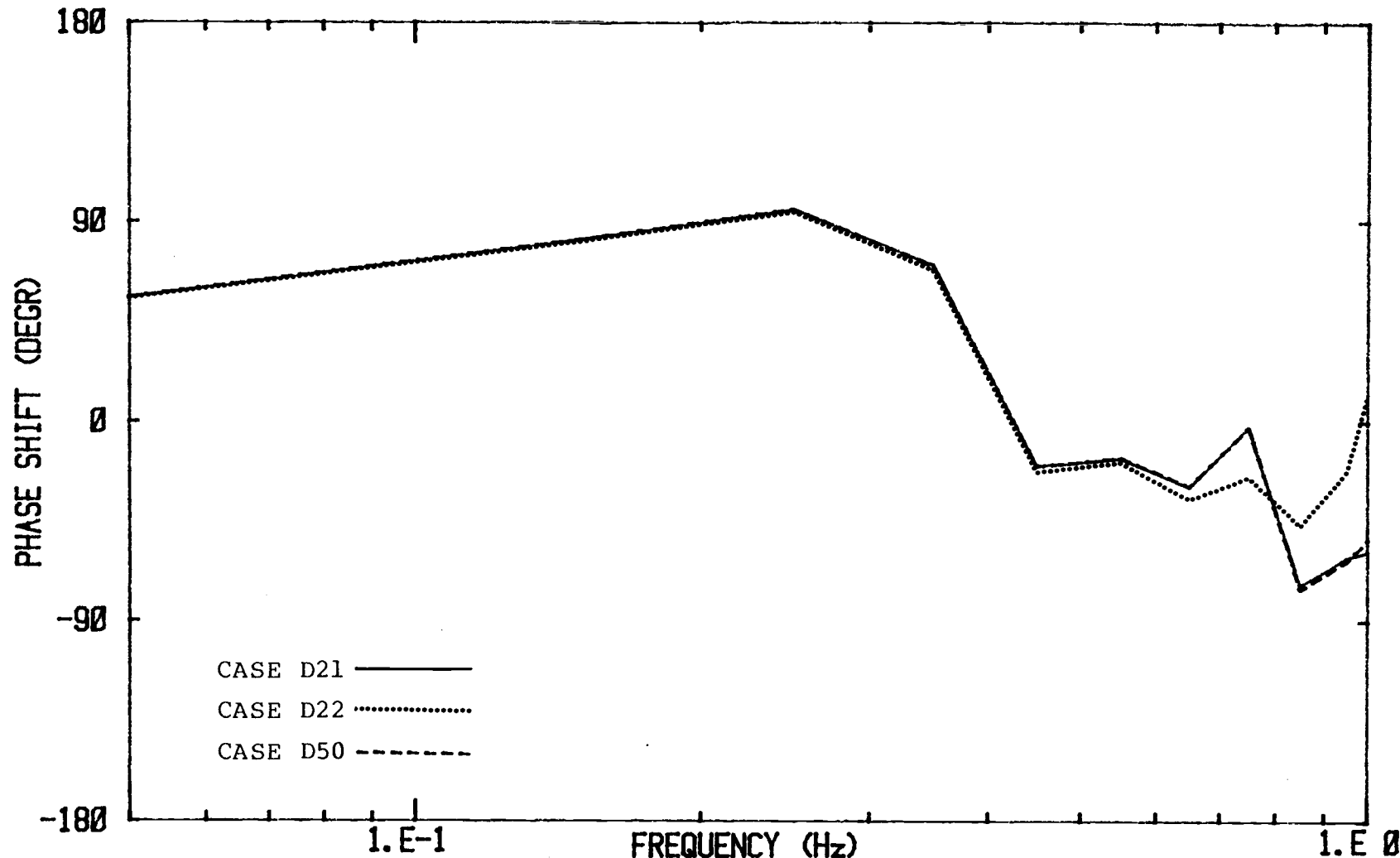


Figure 7. Phase shift of pressure-to-flux transfer function obtained from simplified RETRAN model using constant steam dome qualities of 0.99998 and 0.0.

### II.2.3. "Infinite" Volume Model

A special modeling option exists in the RETRAN code which treats very large volumes ( $>10^9$  ft.<sup>3</sup>) in a manner which differs from that in which normal sized volumes are treated. Specifically, the energy and mass conservation equations are ignored for that volume. Since in the simplified model there is no way for mass to exit the steam dome, it was thought that by using a large volume as a sink, effects caused by mass imbalance in the steam dome could be avoided and the effect would approach that of a true pressure boundary condition.

Three cases were run to examine the effect of the "infinite" volume model on the response calculated by the RETRAN code. Table #3 lists the important steam dome dimensions and decay ratios of the cases for comparison. Case D19 uses the standard steam dome volume from the comprehensive model while in case D20 the steam dome volume is increased to  $10^9$  ft<sup>3</sup>. Comparison of the transfer function of these two cases (figures #8,#9) shows that they agree fairly well in the lower frequencies but are noticeably different at higher frequencies. The decay ratio for the "infinite" volume case is also larger than that of the normal volume case.

Examination of cases D19 and D20 showed that for time dependent volumes, regardless of size, the conservation of mass and conservation of energy equations are ignored. The momentum equation, however, is applied at the junctions which connect the volumes<sup>8</sup>. It is the momentum equation which is responsible for the difference between cases D19 and D20. Changing the steam dome volume to a large value while maintaining the same flow area resulted in a long flow length for the steam dome. This flow length is used in the momentum equation to calculate the friction loss across the junction. Case D21 is a rerun of case D20 with the steam dome flow area adjusted to give the same flow length in the steam dome as in case D19. The results from case D21, also shown in table #3 and figures #8 and #9, are almost identical to those of the standard volume case, D19.

Thus it can be concluded that either the "finite" or "infinite" volume option may be used in conjunction with the time dependent volume and the results will be the same so long as the flow lengths associated with the volumes are equivalent.

CASE	D19	D20	D21
VOLUME (FT <sup>3</sup> )	4786.2	1.0 E9	1.0 E9
FLOW AREA (FT <sup>2</sup> )	343.617	343.617	7.18 E7
FLOW LENGTH (FT)	13.929	2.91 E6	13.9295
DECAY RATIO	.46613	.50588	.46676

Table 3. Steam dome geometry and decay ratios for finite and "infinite" volume models.

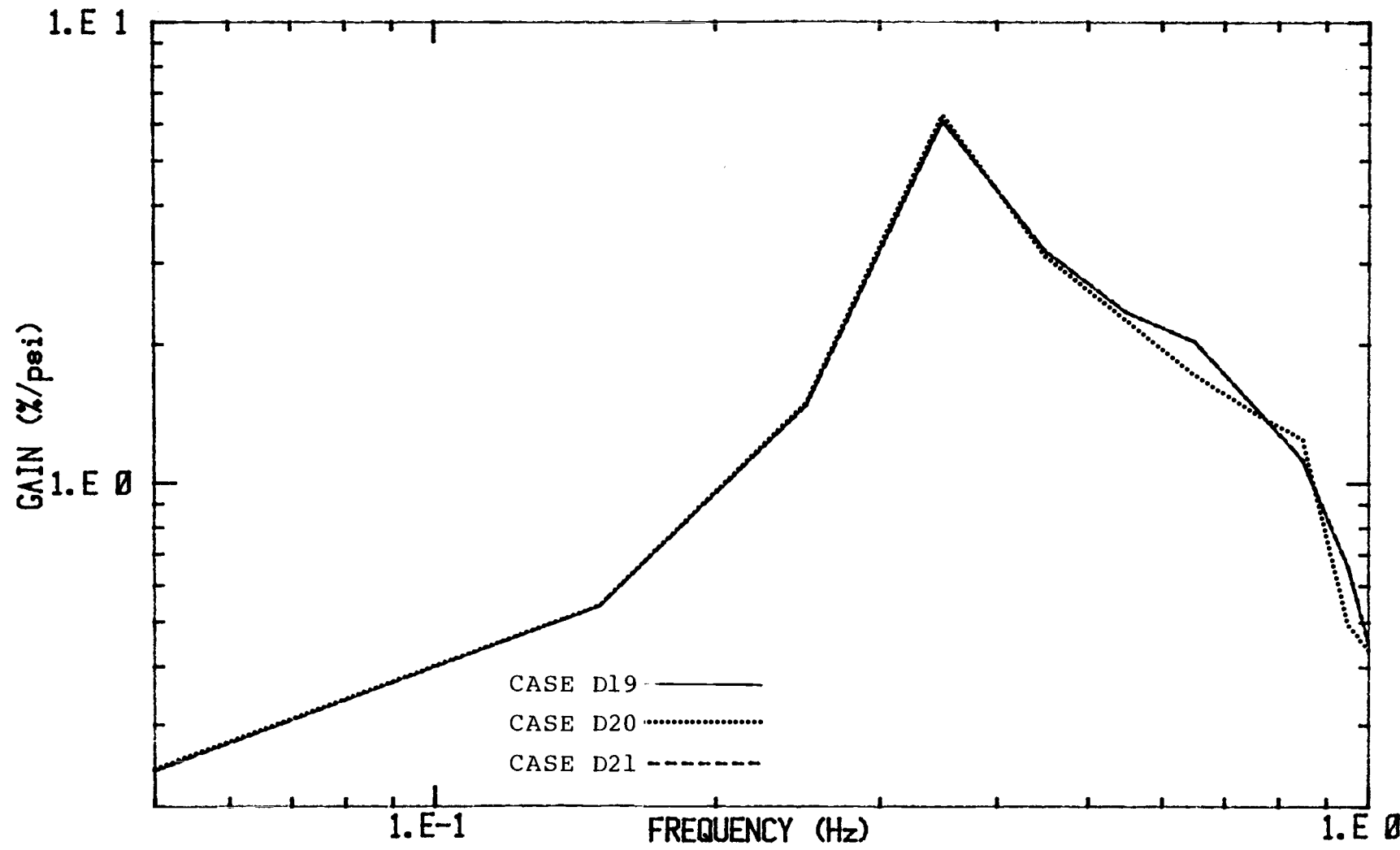


Figure 8. Gain of pressure-to-flux transfer function obtained from simplified RETRAN model using various steam dome dimensions.

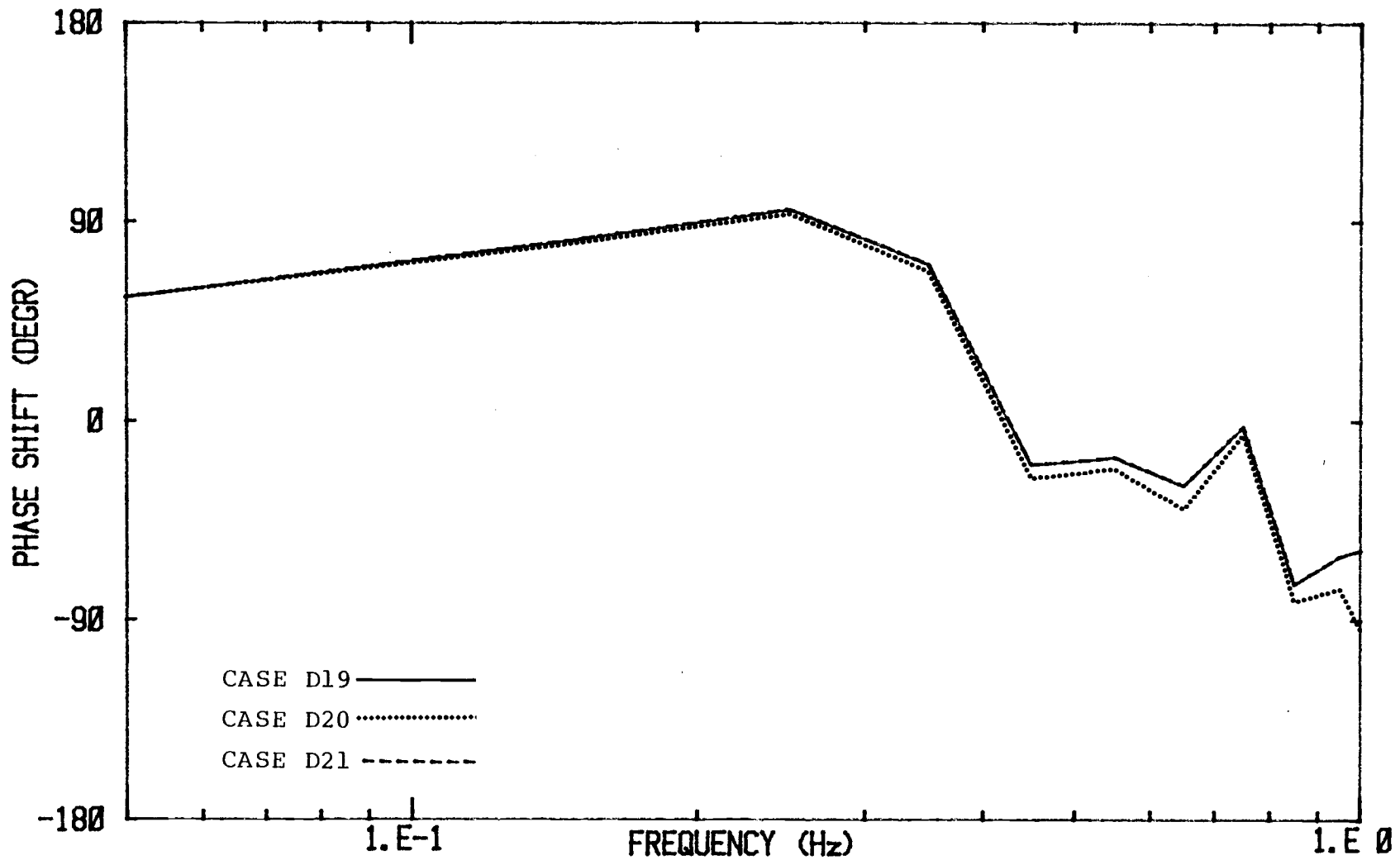


Figure 9. Phase shift of pressure-to-flux transfer function obtained from simplified RETRAN model using various steam dome dimensions.

### II.3. Comparison of Simplified and Comprehensive Models

The aim of the first part of this study was to show that the simplified version of a RETRAN BWR model produces results that are essentially equivalent to those of the comprehensive model and also to demonstrate that the model behaves in a linear manner when small perturbations are used.

The following method was used to compare the comprehensive and simplified models. First, a case was run using the comprehensive model and the transfer function and decay ratio were calculated. The steam dome pressure transient from this case (fig. #10) was then input into the simplified model, using the method described in the previous sections, and a transient case was run. Plots of the system normalized power and the transfer function for cases S56 (comprehensive model) and D52 (simplified model) are shown in figure #11 and figures #12 and #13 respectively. The decay ratio for case S56 is 0.408 while that of case D52 is 0.448.

Both the gain and the phase shift curves for the two cases have the same general shapes. The gain plots are essentially the same in the lower frequency range. At frequencies above .35 Hz the comprehensive model produces gains which are larger than those of the

simplified model. The phase shift is slightly larger for the comprehensive model, with the difference in phase shifts between the transfer functions increasing with the frequency.

The small difference in the transfer functions is due to the non-linearity of the models and arises because the perturbation functions used in the two models are not exactly the same. In the simplified model the pressure signal is represented by 64 data points separated by a constant time interval,  $\Delta t$ . The actual integration time step used in the code to perform the calculations is smaller than  $\Delta t$  and the code interpolates linearly between the data points to obtain the steam dome pressure for each time step. In the comprehensive model the pressure is determined by the model equations at each time step. As a result of the difference in the way the code determines the pressures in the comprehensive and simplified models, the steam dome pressure signals for the two models are slightly different between the 64 points the signals have in common. These differences are in frequency components which are higher than those used in the analysis, but because of the non-linearity of the models they affect the response at all frequencies to some extent. Another difference in the signals is that the quality in the steam dome is held constant in the simplified model, but

is allowed to vary in the comprehensive model. As a result the models actually represent two slightly different systems.

The same transfer functions should be obtained for a linear system regardless of the perturbation function used. The RETRAN model does not represent a truly linear system, but if certain constraints are placed on the perturbation function the assumption of linearity may be made when performing the frequency domain analysis. To demonstrate the validity of the linearity assumption, a pressure perturbation function was synthesized following the constraints described in the previous sections. A case was then run with this perturbation in the simplified model and the results were compared with those obtained from the simplified model using the perturbation function from the comprehensive model. The synthesized pressure function is plotted in figure #10 with the steam dome pressure signal from the comprehensive model. The transfer function obtained from this case is plotted in figures #12 and #13 along with those from the comparison of the comprehensive and simplified models.

The gain and phase shift curves obtained are identical up to .55 Hz. At higher frequencies some discrepancies occur, giving an indication of the lack of

resolution in this range. The results of this comparison verifies the validity of the linearity assumption at least for frequencies below .55 Hz.

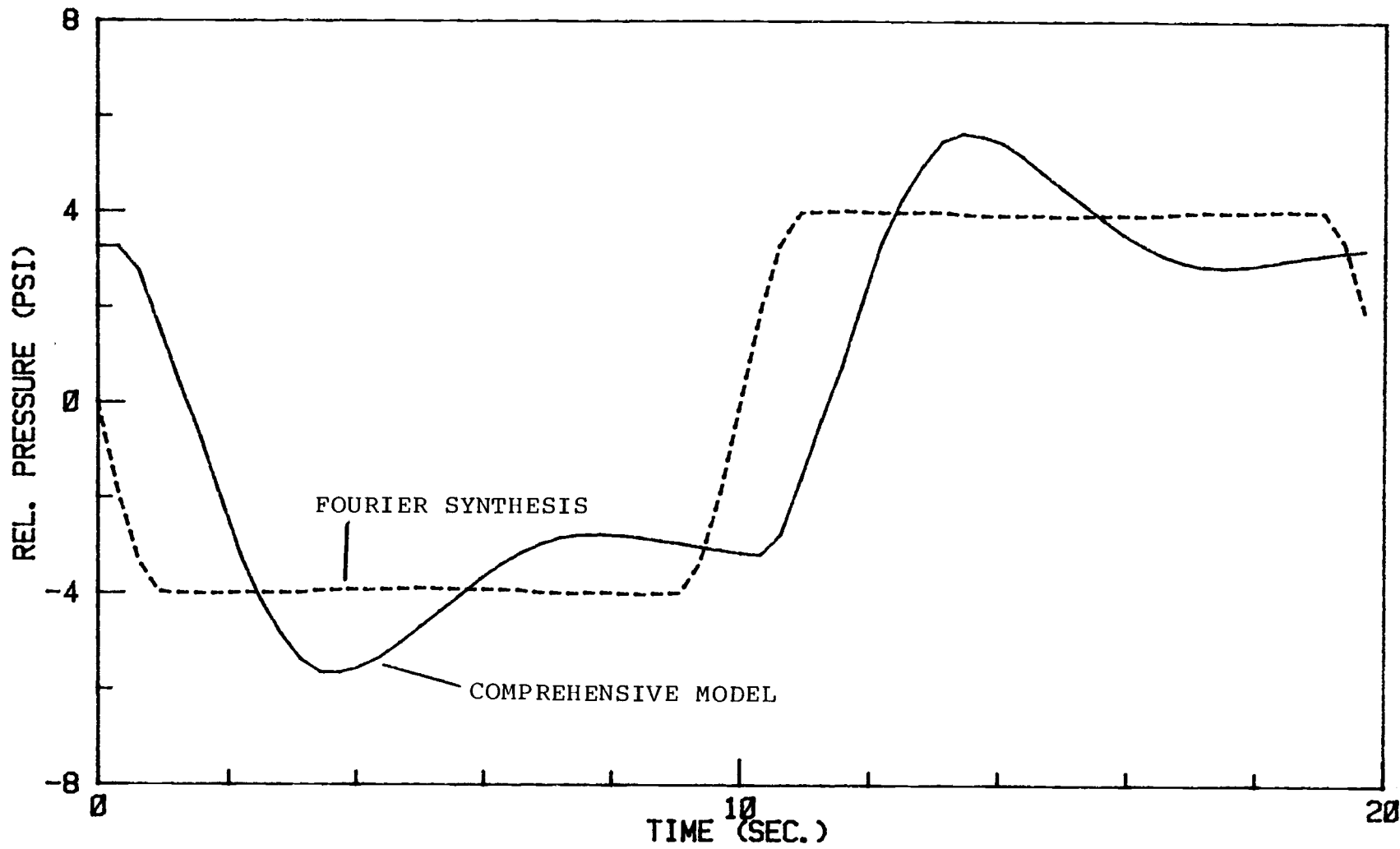


Figure 10. Steam dome pressure transients obtained from the comprehensive RETRAN model and by Fourier synthesis.

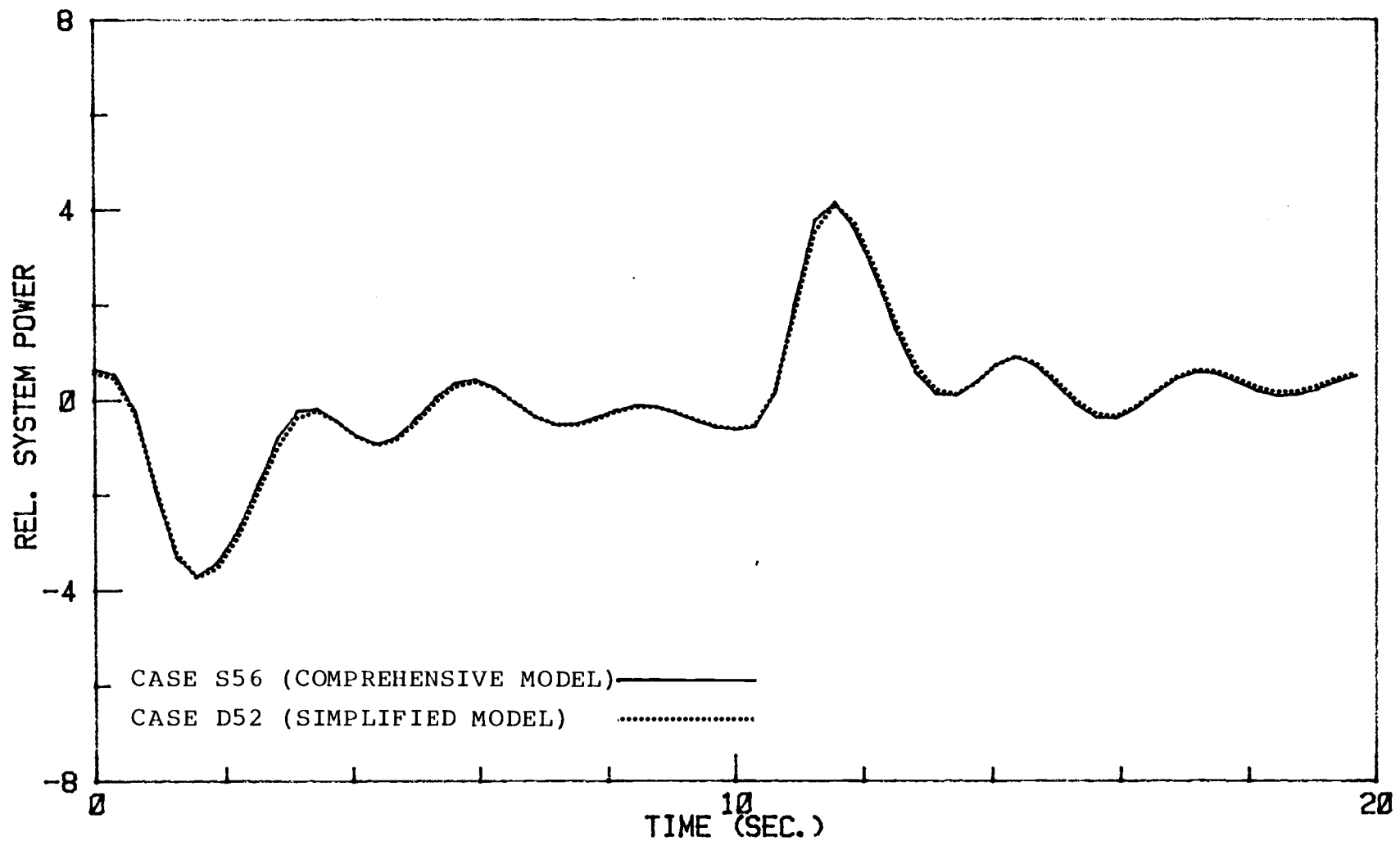


Figure 11. Calculated power transients obtained from comprehensive and simplified RETRAN models.

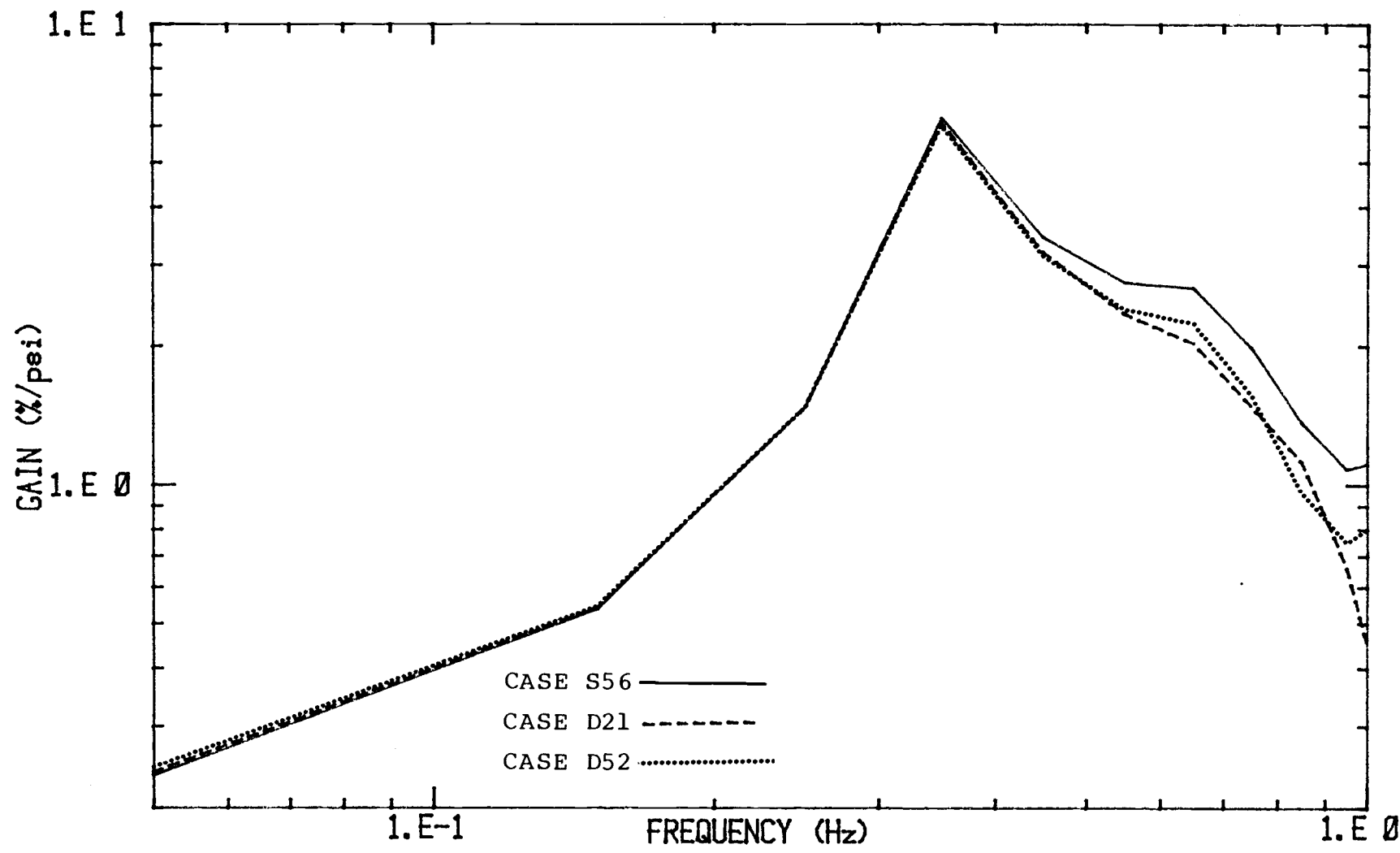


Figure 12. Gain of pressure-to-flux transfer function obtained from comprehensive and simplified RETRAN models.

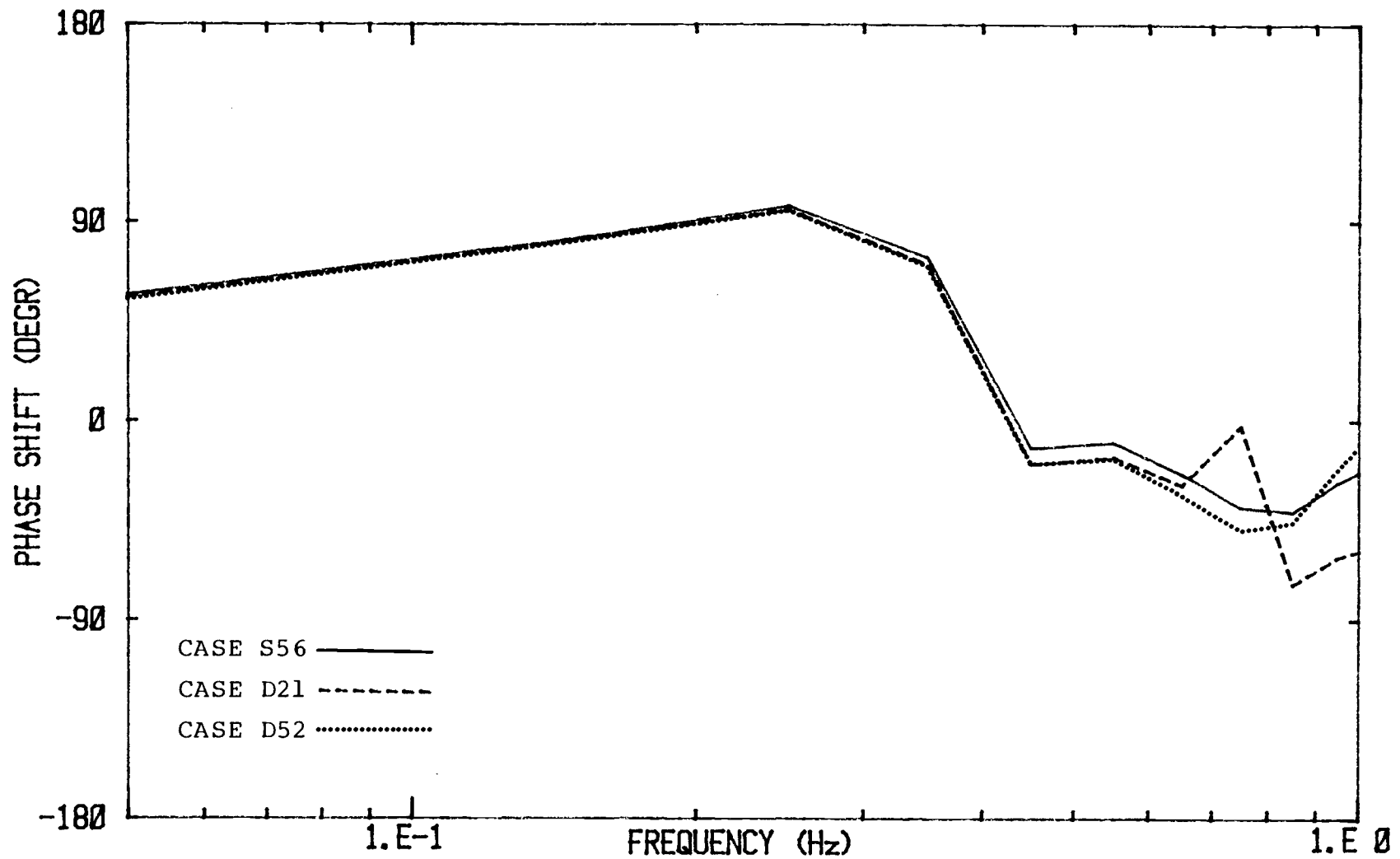


Figure 13. Phase shift of pressure-to-flux transfer function obtained from comprehensive and simplified RETRAN models.

### III. PARAMETRIC STUDIES PERFORMED UNDER NATURAL CIRCULATION CONDITIONS

Since no tests were performed at PB2 under natural circulation cooling conditions, there is no data for comparison with the calculated results from the RETRAN models in this case. On the other hand, there are indications that the system exhibits the least margin with respect to the stability limits when operating under natural circulation conditions. Therefore, these conditions were investigated in some detail with the existing RETRAN model. Also, the sensitivity of the calculated results to several modeling options and systems parameters was examined under these conditions. They are the jet-pump model, the homologous pump head curves, the two-phase-flow models, the axial power profile, and the reactor power level.

#### III.1. Determination of Steady State Natural Circulation

Before the simplified RETRAN model could be used to examine a transient case under natural circulation cooling a consistent steady state solution had to be determined. Under natural circulation the driving force behind the core flow is due to the coolant density

difference between the rising (heated) section and the downcomer of the flow loop, rather than due to the action of the jet pumps<sup>9</sup>. In order to model this condition with the simplified RETRAN model the recirculation pump speed is set to a very low value. Initial attempts to use a pump speed of 0.0 failed because of coding features which precluded this special case. Instead, a pump speed of .1668 rpm (.01% of rated speed) was used for these studies. The core flow must also be adjusted in order to obtain a steady state solution for natural circulation which is consistent with that for forced convection. Another important system parameter, axial power profile, was not adjusted in the change from forced convection cooling to natural circulation cooling but was examined in the parametric studies.

### III.1.1. Flow Boundary Conditions

The flow boundary conditions for natural circulation steady state were set by assuming that the reactor was at the same power level as in the forced convection case, and that steam would enter the steam dome at the same conditions and at the same rate as in the forced convection case. Feed water would have to enter the system at the same rate as in the forced

convection case in order to maintain a constant mass of coolant in the system.

### III.1.2. Internal Flow Conditions

For the model under natural circulation conditions to be consistent with the model under forced convection two more conditions need to be satisfied. The carryunder from the steam separators must be small (less than .5%) and the unspecified loss coefficient associated with each flow loop in the model must be the same as in the forced convection case. The first condition is based on the actual performance of the steam separators. It was met by adjusting the enthalpy specified for the coolant in the lower plenum. The second condition is based on the definition of the loss coefficients. In the RETRAN code, one loss coefficient must be left unspecified in each flow loop. This unspecified loss coefficient is computed by the RETRAN code during steady-state self-initialization so that a closed pressure profile is obtained around the flow loop. By definition, however, the loss coefficients are functions only of geometry, and should be the same under all conditions of reactor operation<sup>10</sup>. The unspecified loss coefficients were set to the desired values by adjusting loop mass flow rates and volume coolant levels as indicated in table #4.

FLOW LOOP	LOSS COEFFICIENT	PROCESS PARAMETER ADJUSTED
Core/downcomer	$K_{13}$ *	Jet pump suction flow
Recirculation	$K_{14}$	Jet pump drive flow
Core/bypass	$K_{33}$	Core bypass flow and core coolant flow
Steam separator interior-exterior	$K_{38}$	Steam separator exterior water level

Table 4. Process parameters used to adjust unspecified loss coefficients.

---

\* The unspecified loss coefficients belong to the junctions which connect the following volumes:  
 $K_{13}$ : upper downcomer (#12) to jet pump (#13)  
 $K_{14}$ : recirc. line (#19) to jet pump (#13)  
 $K_{33}$ : lower plenum (#1) to core by pass (#30)  
 $K_{38}$ : steam separator (#9) to steam dryer (#35)

### III.2. Recirculation System Model

The recirculation system model used in the RETRAN model can be thought of as consisting of two parts, the jet pumps and the recirculation pumps. The jet pump itself is modeled through the arrangement and geometrical specification of several RETRAN volumes and use of a special momentum mixing option. For the recirculation pump, a centrifugal pump which drives the jet pump flow, a set of homologous pump curves are used to describe the affect of the pump on the coolant. The sensitivity of the transient response with regard to both the jet pump geometry and the homologous pump curves was examined.

#### III.2.1. Jet Pump Geometry

The jet pump model used in the simplified RETRAN model is based on one dimensional momentum mixing of two flows. Figure #14 shows a generalized RETRAN geometry of the jet pump model. In this model the downcomer is considered as the suction volume, another volume is used to represent the drive line, and a third control volume is used to represent the mixing section and the diffuser.<sup>11</sup>.

The important consideration in this model is that of the flow areas of the junctions which connect these three volumes, as they represent the drive, suction, and mixing section flow areas used in the momentum equations. The mixing section area,  $A_m$ , is not modeled separately in this technique, and instead is taken to be the sum of the suction and the drive flow areas,  $A_s$  and  $A_d$ . For the case of forced convection the drive flow area and the mixing flow area are the most important in the solution of the momentum mixing equation so their true geometrical areas are used. The suction flow area is then defined as:

$$A_s = A_m - A_d \quad (1)$$

For the case of natural circulation cooling the drive and mixing flow areas take on less importance because the momentum transfer between the drive and suction flows is no longer the driving force behind the core flow. Instead, the coolant flow is caused by density differences between the coolant in the core and downcomer regions. A much greater portion of the total core flow passes through the suction flow area under these conditions and the suction flow area becomes more important.

To assess the importance of the suction flow area for the transient behavior, the flow area was increased by 10% over that used in the natural circulation base case. In order to isolate the effect of the change in the suction flow area from that of the total core flow, the initial flow was kept at the rate used in the base case. The initial division of flow between the drive and suction lines was determined by maintaining the computed loss coefficient in the drive line at its base case value. This criteria for determining the flow division is based on the definition of the loss coefficient as a geometrical factor which does not change with flow rate. The comparison of the transfer functions of these two cases, figures #15 and #16, indicate that the results are insensitive to changes in the suction flow area, as considered here.

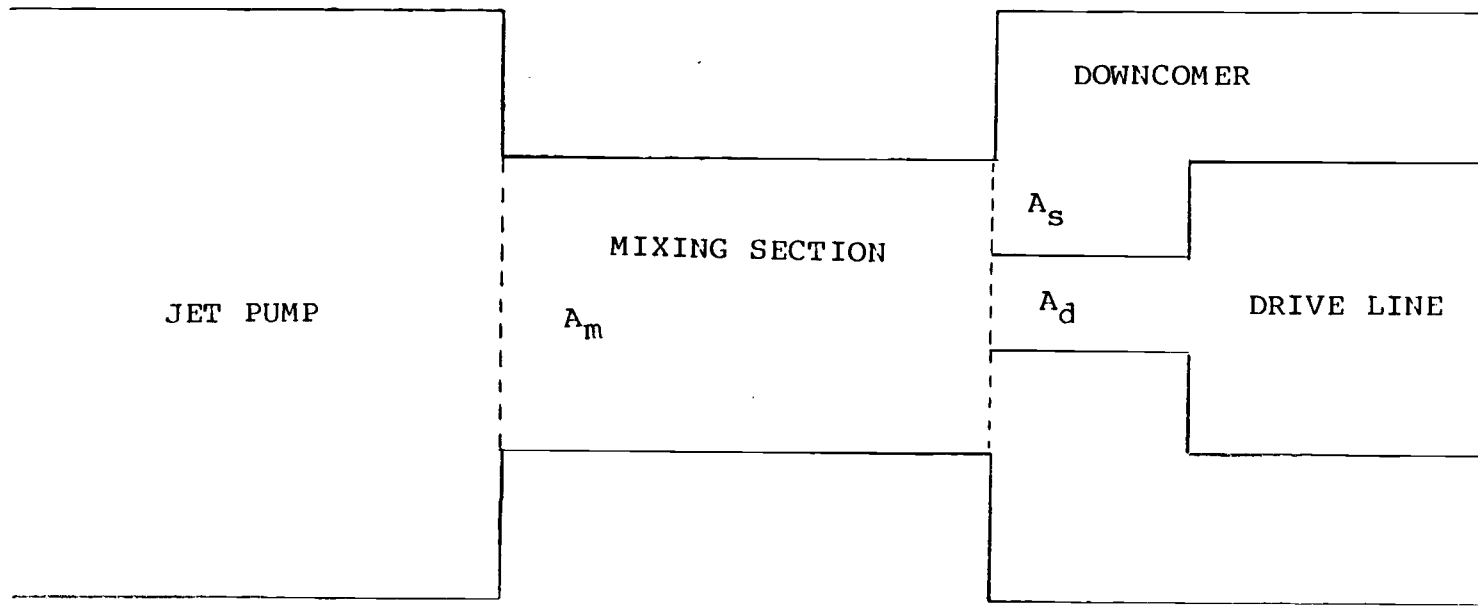


Figure 14. Schematic diagram of RETRAN jet pump geometry.

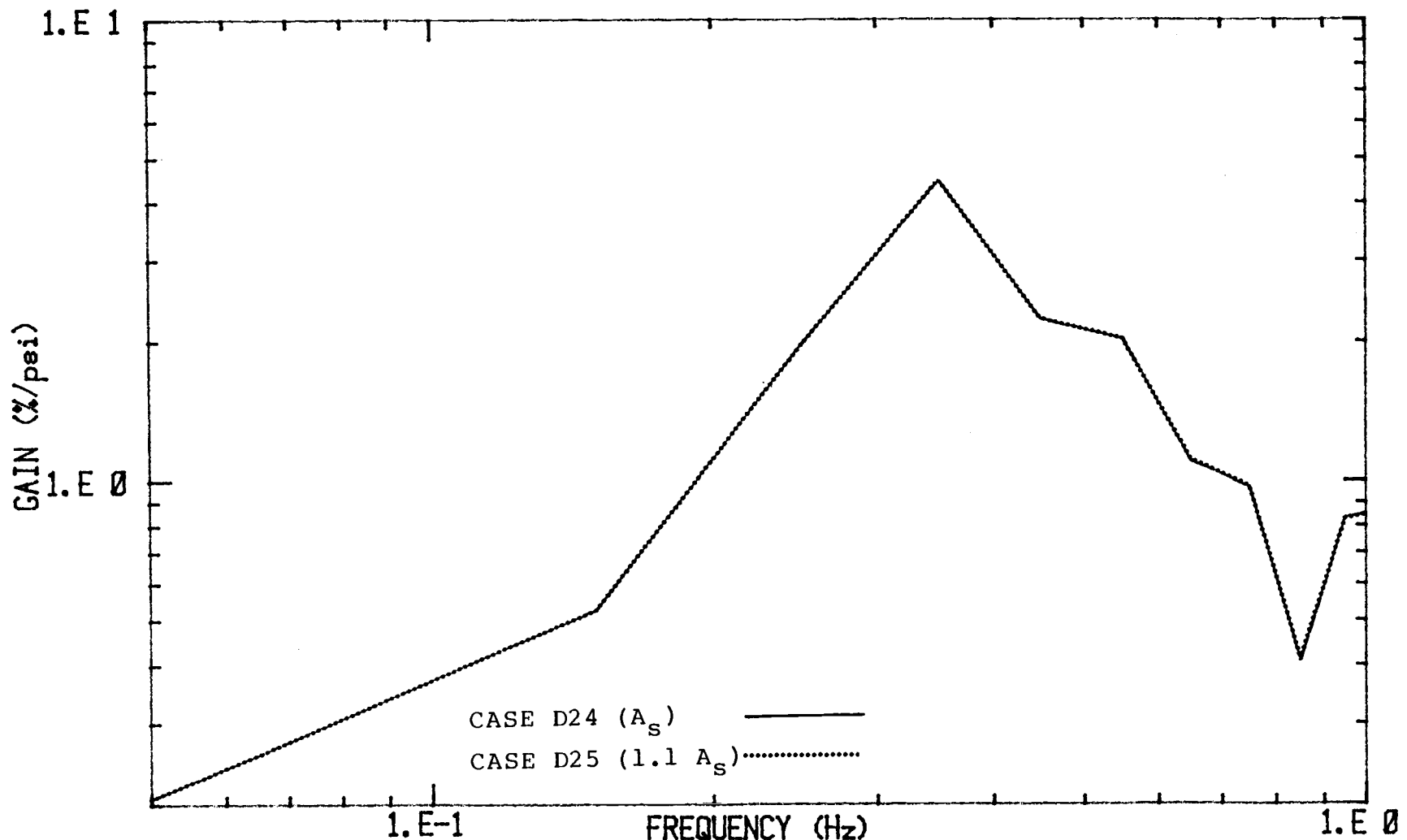


Figure 15. Gain of pressure-to-flux transfer function obtained from simplified RETRAN model for various values of the jet pump suction flow area.

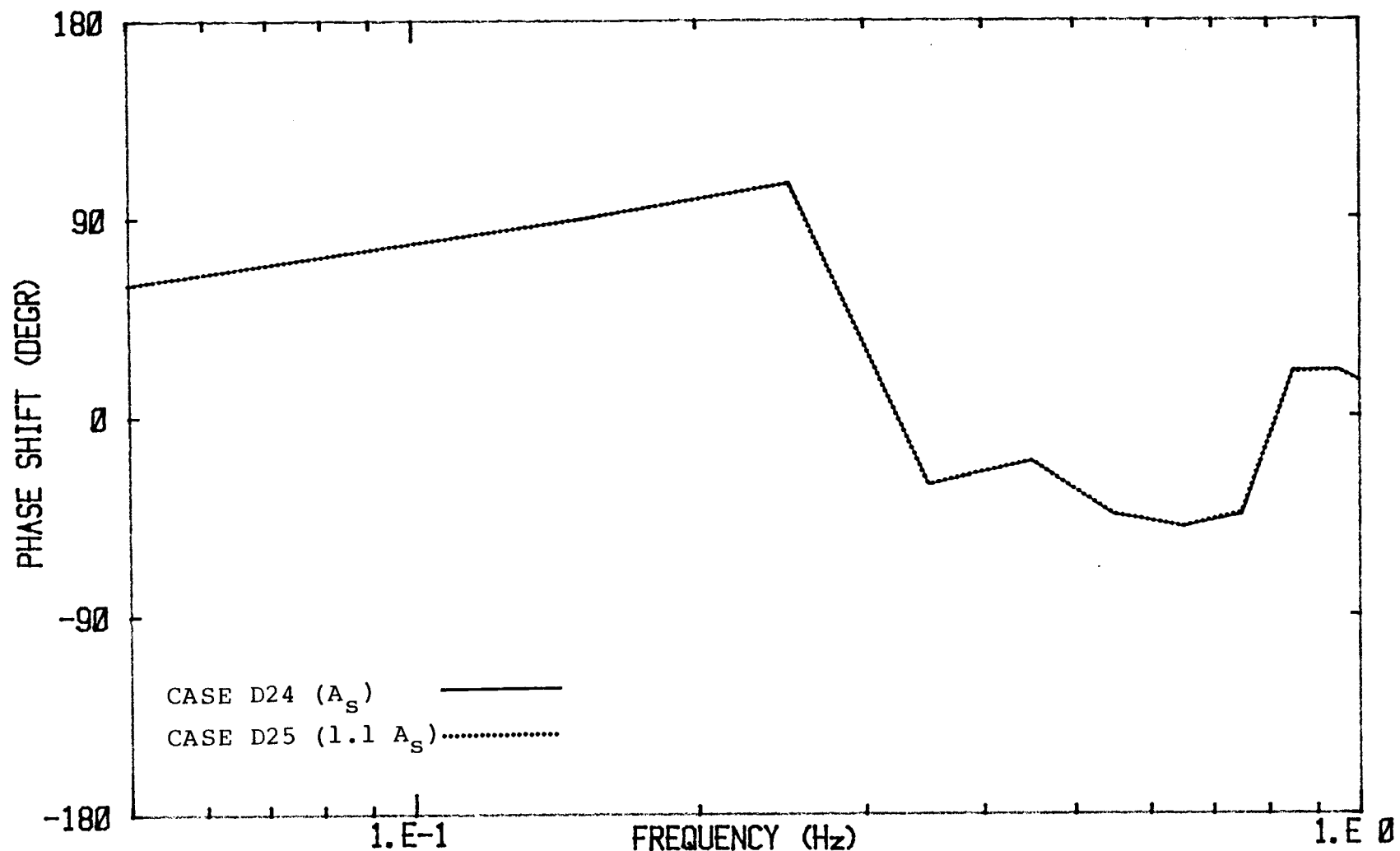


Figure 16. Phase shift of pressure-to-flux transfer function obtained from simplified RETRAN model for various values of the jet pump suction flow area.

### III.2.2. Homologous Pump Curves

In order to model the interaction between the centrifugal pump and the coolant, a set of pump characteristic curves must be supplied to RETRAN. The homologous pump head curves define the relation between the pump head and the volumetric flow rate and pump speed using a dimensionless formulation.

The pump curves used in the comprehensive model did not extend into the low pump speed/flow ratio region as needed to model natural circulation conditions. More extensive curves were obtained from reference<sup>12</sup>, but an extrapolation was still necessary to cover the region near zero pump speed. This extrapolation introduced some amount of uncertainty into the model. To assess the sensitivity of the stability characteristics of the system to the homologous pump head curves, a comparative transient calculation was performed using a significantly different extrapolation of the curve. Both the reference curve and the alternate extrapolation are shown in figure #17.

The homologous pump head curves are plotted as  $h/v^2$  vs.  $a/v$  where

$a$  = ratio of actual to rated pump speed

v = ratio of actual to rated pump flow rate

h = ratio of actual to rated pump head

The effect that the alternate extrapolation had on the model was one of increasing the head loss experienced by the flow through the pump at zero speed. As a result, the flow rate through the pump was reduced, which in turn reduced the total core flow rate. The results of transient cases performed with the different pump curves are compared in table #5 and figures #18 and #19.

Two conclusions can be drawn from the results of these two cases. First, the sensitivity of the calculated transient response to the homologous pump head curves, under natural circulation conditions, is small. Second, the RETRAN model predicts a reduction in system stability as the coolant flow to the core is reduced while maintaining a constant power level.

CASE	D24	D36
Suction flow (lbm/sec)	7470	7450
Drive flow (lbm/sec)	1239	1045
Core flow (lbm/sec)	8709	8495
Decay ratio	.602	.635

Table 5. flow rates and decay ratios obtained for various extrapolations of the RETRAN homologous pump head curves.

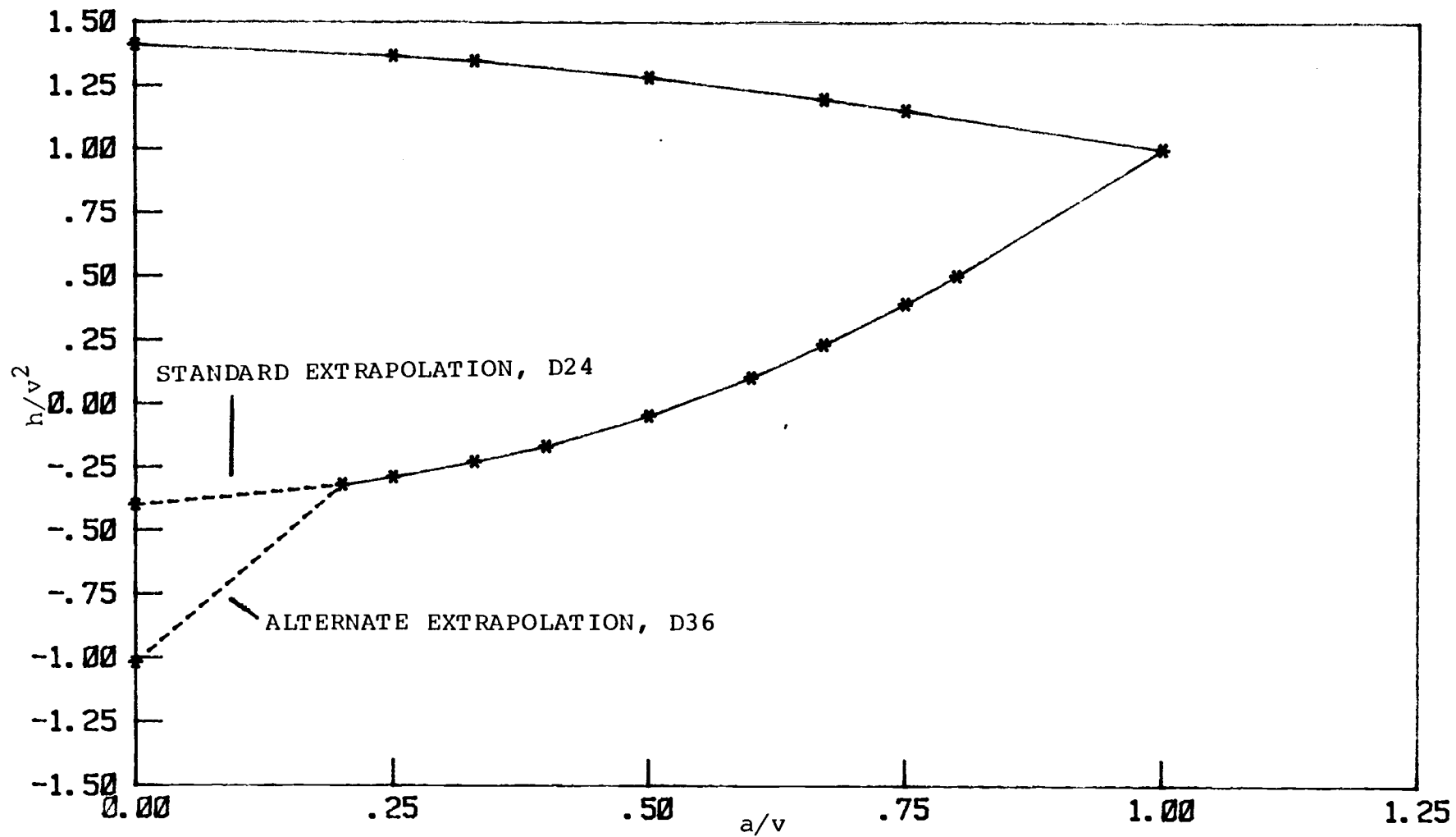


Figure 17. Homologous pump head curves used in simplified RETRAN model.

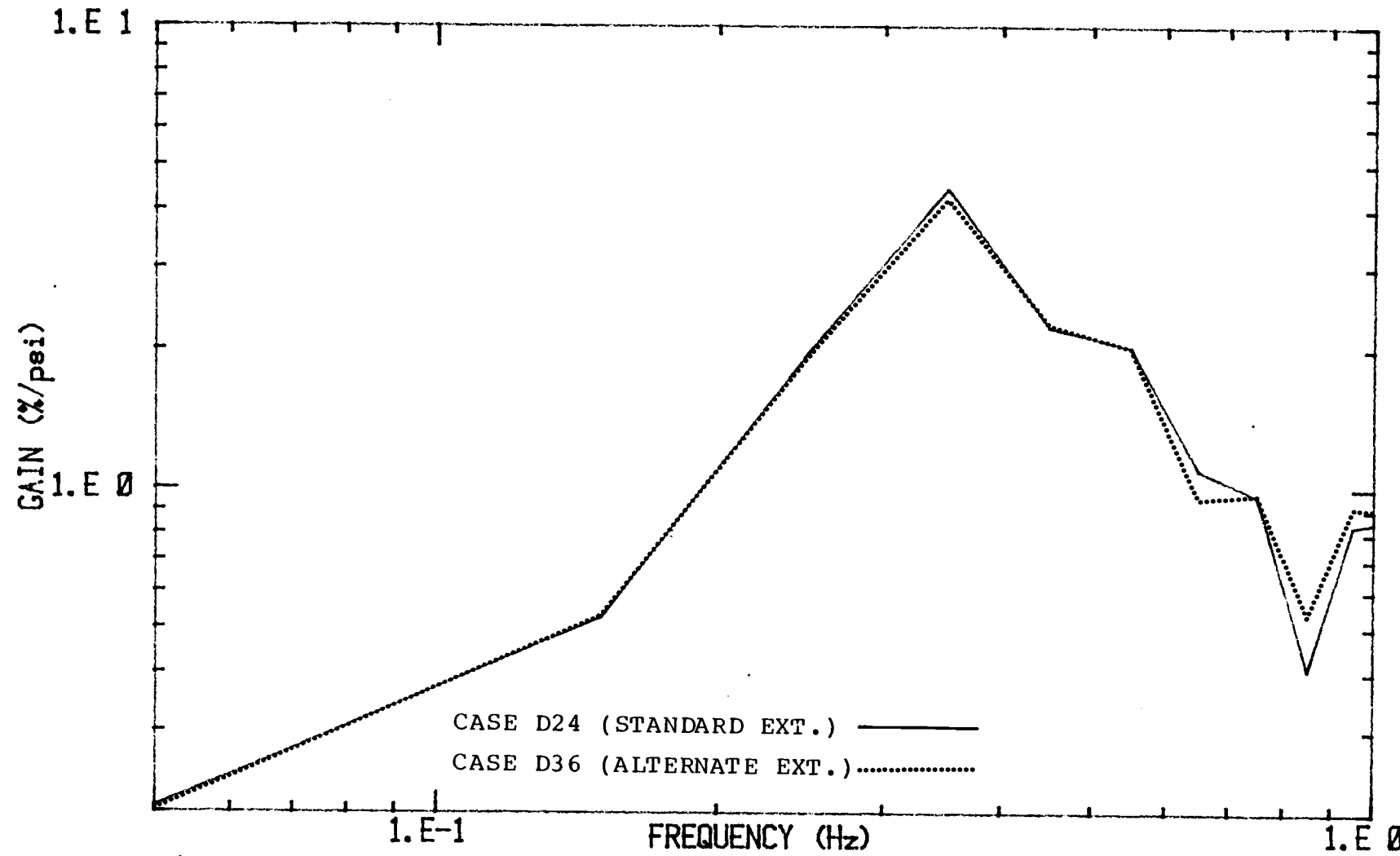


Figure 18. Gain of pressure-to-flux transfer function obtained from simplified RETRAN model using various extrapolations of homologous pump head curves.

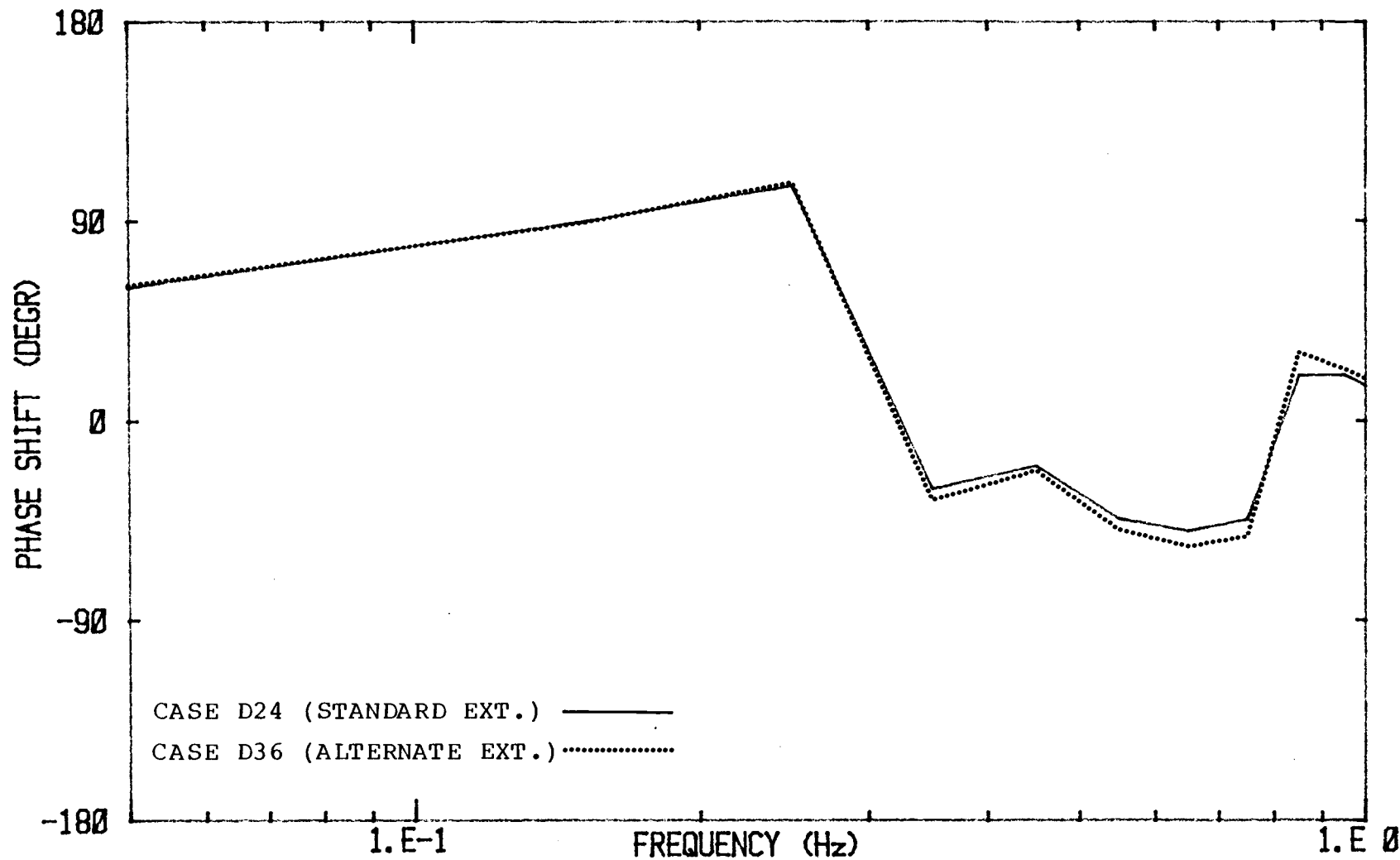


Figure 19. Phase shift of pressure-to-flux transfer function obtained from simplified RETRAN model using various extrapolations of homologous pump head curves.

### III.3. Two-Phase-Flow Models

Three two-phase-flow models are available in the RETRAN code: the dynamic slip model (DSM), the algebraic slip model (ASM), and the homogeneous equilibrium mixture model (HEM). The DSM was not used in the comparison of two-phase-flow models because of difficulties encountered in its use. The ASM for two-phase-flow was used in all cases examining other parameters in this study. Comparison of the ASM and the HEM showed that the two phase flow model which was used had a significant effect on the resulting transient calculation. A comparison of normalized reactor power for similar cases (figure #20), one using ASM and one using HEM, shows that the HEM case diverges.

The divergence of the case using the HEM is caused by enhancement of the void reactivity feedback mechanism. The void fraction for both models is given by the relation:

$$q = \frac{1}{\left(\frac{1-x_f}{x_f}\right) \cdot \left(\frac{\rho_g}{\rho_l}\right) \cdot H + 1} \quad (2)$$

where

$x_f$  = flow quality

$\rho_g$  = density of vapor phase

$\rho_l$  = density of liquid phase

and  $H$ , the slip ratio is defined as:

$$H = V_g / V_l \quad (3)$$

where

$V_g$  = velocity of vapor phase

$V_l$  = velocity of liquid phase

For the HEM the slip ratio is equal to 1 by definition, while in the ASM the slip ratio will be greater than 1. This means that the void fraction will be smaller when the ASM is used. In figure #21 plots of the steady state axial void distribution for similar cases, one using the HEM and the other using the ASM, demonstrate the difference in void fraction associated with the two models. This plot also shows that in the one phase region the two models yield the same results, as would be expected. Correspondingly there is a greater change in void fraction with change in power in the case of the HEM, particularly near the boiling boundary, which leads to the reduction in stability. This difference in the change in void fraction per change in power for the two models shows up in the coolant density oscillations in the core. The density in volume #5, for cases using either model, is plotted vs. time in figure #22. The density oscillations decay slowly in the case employing the ASM but diverge for the HEM case.

The comparison of the ASM and HEM two phase flow models suggest that the HEM is a more conservative model while the ASM is better for "best estimate" calculations. The two-phase-flow-model study also demonstrated the ability of the RETRAN code to model the non-linearities associated with a nuclear reactor system. When the perturbation is discontinued in the unstable cases using the HEM option the calculated transient approaches a limit cycle, figure #23, which is a property of non-linear systems<sup>13</sup>.

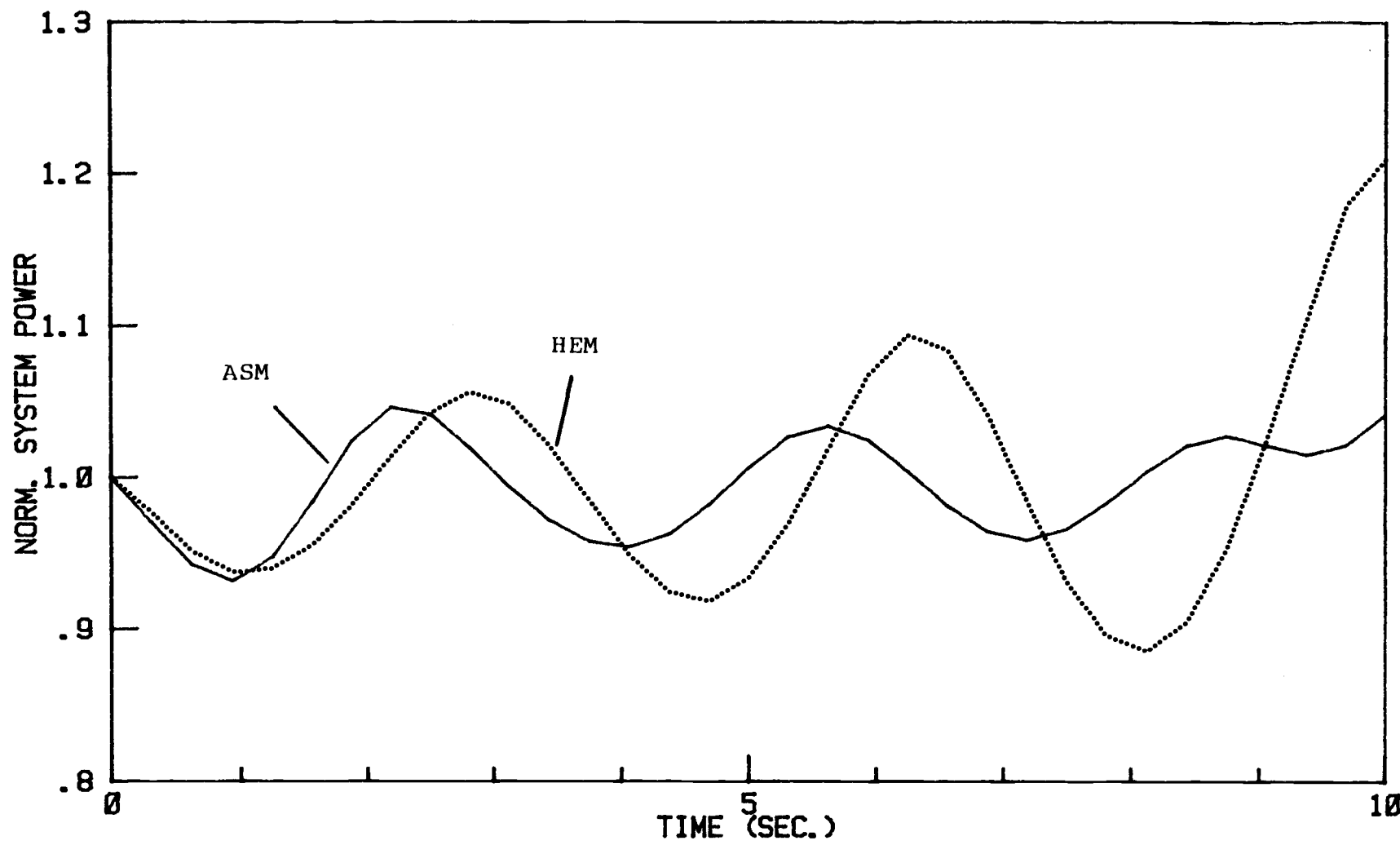


Figure 20. Reactor power transients for HEM and ASM for two-phase-flow.

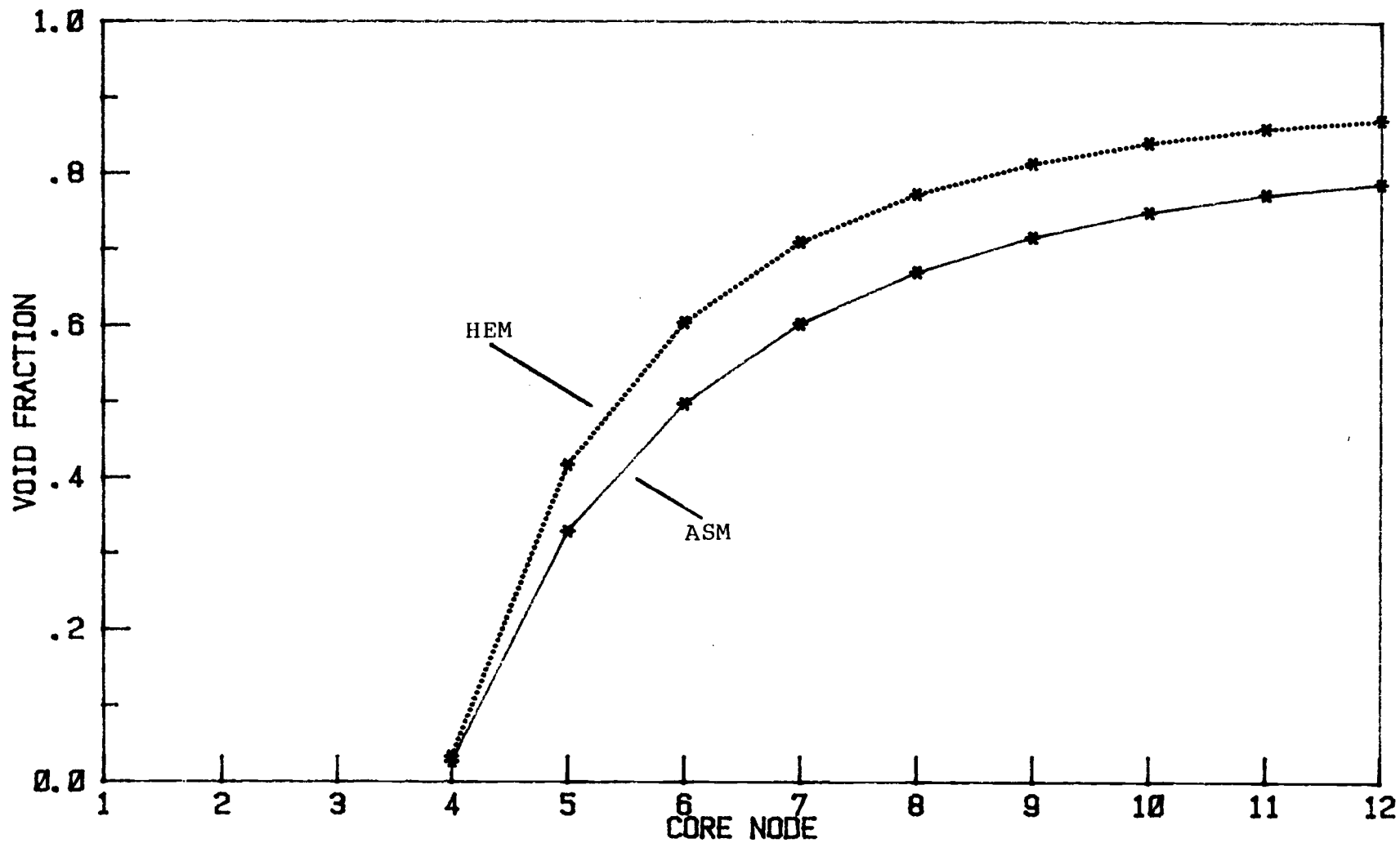


Figure 21. Axial distribution of coolant void fraction at steady state for HEM and ASM for two-phase-flow.

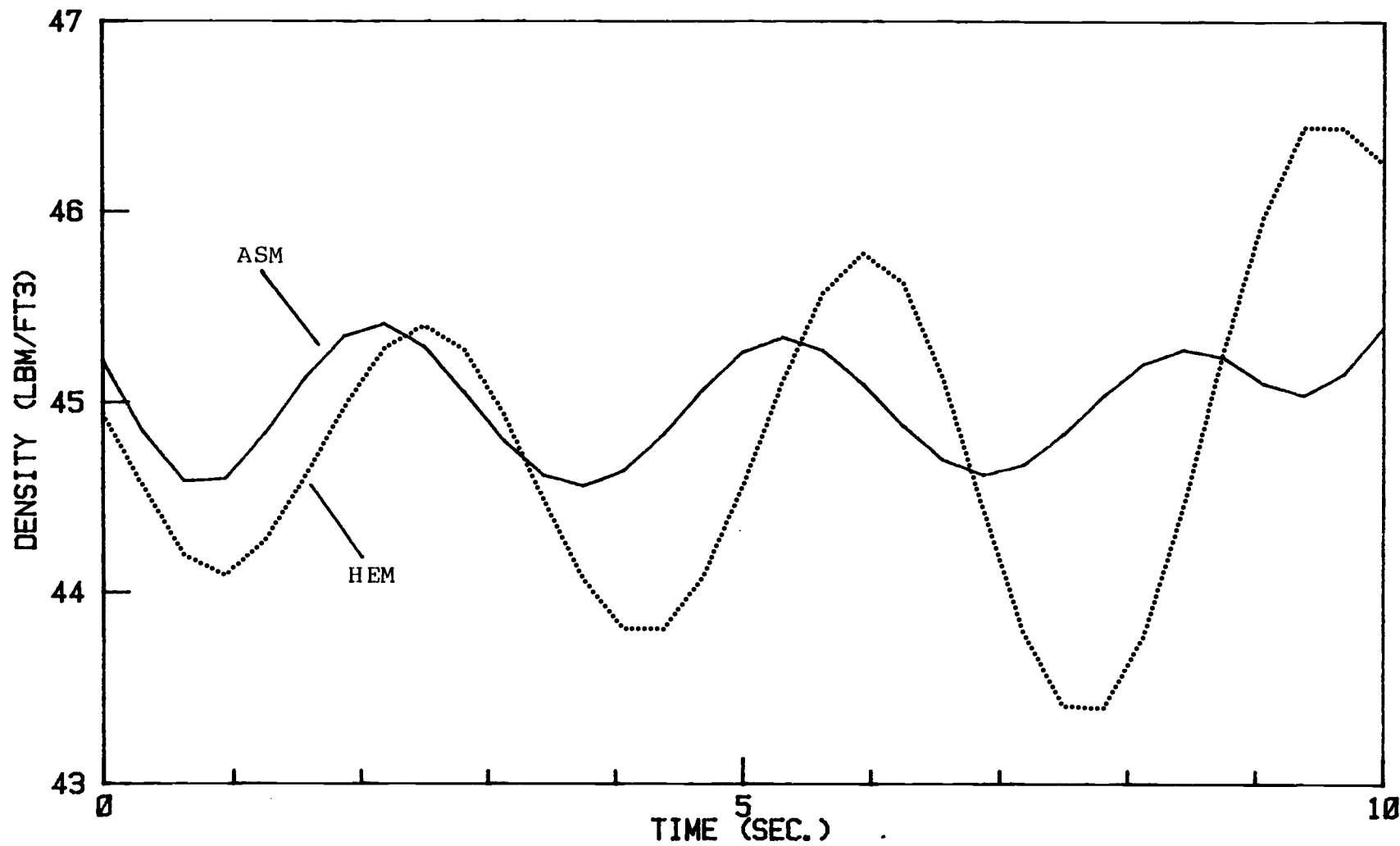


Figure 22. Density transients for HEM and ASM for two-phase-flow.

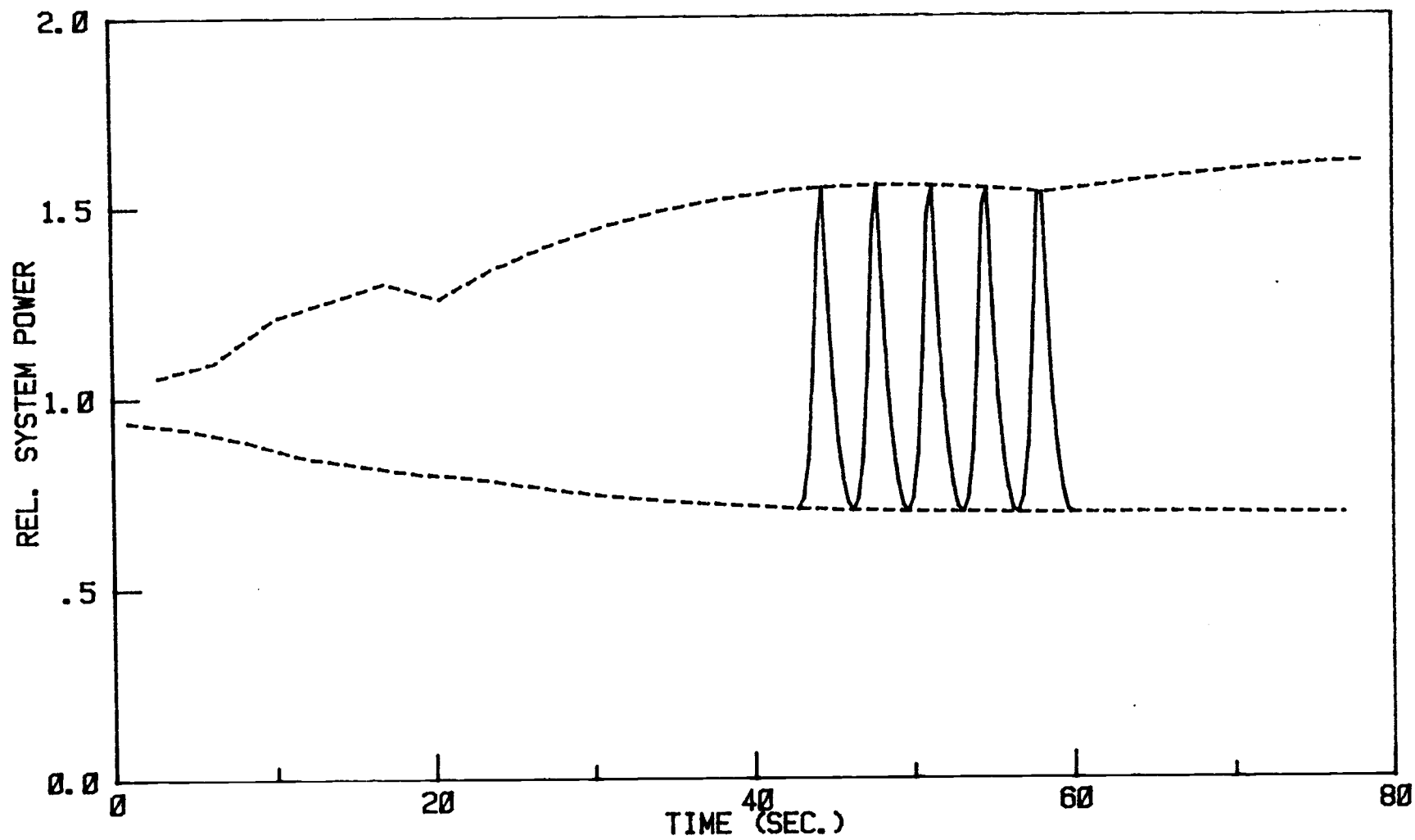


Figure 23. Reactor power transient limit cycle calculated using HEM for two-phase-flow.

### III.4. Natural Circulation at Full Power

Operating experience suggests that the stability of a BWR under natural circulation cooling conditions should decrease as the power level increases. To determine whether the RETRAN model would show this effect the initial steady power level was raised from the reference level ( 1948 MWth, corresponding to 58.45% of full power of the Peach Bottom plant) to 100% power (3332.76 MWth). Again, before transient calculations could be performed the flow boundary conditions, loss coefficients, and carryunder had to be adjusted in order to keep the model consistent with the previous cases. The axial power profile would also change in this case, as the control rods would have to be moved to increase the power. Since no exact information is available on what the axial profile would be at full power, the effect of the profile on the results was examined by way of a parametric study.

#### III.4.1. Determining the Steady State

The criteria and methods used for setting the unspecified loss coefficients and steam separator carryunder in order to obtain a consistent steady state at 100% power are the same as those used in going from

forced convection to natural circulation and are described in section III.1.2.. The criteria for the flow boundary conditions are different, however, because of the increased amount of energy which must be removed from the system. The assumption used to set the flow boundary conditions is that steam will enter the steam dome in the same thermodynamic state as at lower power and the mass flow will go up in direct proportion to the increase in reactor power. Again, in order to maintain a system mass balance the feed water influx rate is the same as the steam exit mass flow rate.

### III.4.2. Axial Power Profile/ Nodal Effect

The axial power profile proved to have a significant affect on the transient response of the system, mostly through its influence on the initial position of the boiling boundary relative to the center of the volume in which the boiling boundary is located. Figure #24 shows a schematic representation of several RETRAN volumes and junctions. This figure can be used to describe how the RETRAN model determines the properties it uses for each volume and junction calculation. The figure focuses on that zone of the core in which the boiling boundary is located. The properties associated with the coolant in any volume are taken to be those

which exist at the center of the volume. In the case of determining the quality or void fraction in a core volume, which is then used for void reactivity feedback calculations, this method of equating the average properties of the coolant in a volume to those at the volume center constitutes an approximation which is particularly inaccurate in the volume where the bulk boiling boundary is located.

During a transient the most significant contribution to the change in void reactivity feedback comes from the volume in which the boiling boundary is located. If the actual boiling boundary happens to fall just above the center of a volume, that volume will be treated by RETRAN as if it were all liquid. In this case most of the void reactivity feedback will be lost since the region which most affects it is not accounted for. The other extreme occurs when the boiling boundary falls just below the center of a volume. In this case the large relative changes in void fraction which occur very close to the boiling boundary during a transient are used by RETRAN to describe the conditions in the entire volume. This leads to a situation in which unrealistically high changes in void reactivity is calculated by the code.

The initial positions of the boiling boundaries for two cases, D42 and D46, are indicated in figure #24 and the axial power profiles for these cases are plotted in figure #25. Cases D42 and D46 demonstrate the two extremes of this boiling boundary phenomenon. The axial power profiles for these two case, as shown in figure #25, are almost identical, with that of case D46 being shifted down the core slightly to lower the position of the boiling boundary. The resulting power transient responses for these two extreme cases are shown in figure #26. The response of case D42 (boiling boundary above volume center) is highly damped, while that of case D46 (boiling boundary just below volume center) is unstable and appears to be erratic.

The nodal effect also is present the HEM is used. In figure #27 the system power response for cases D53, boiling boundary just above volume enter, and D54, boiling boundary just below volume center, which used the HEM option are plotted. Again a significant difference in results is seen when only a small change in axial power profile is made.

### III.4.3. Stability at Full Power

The nodal effect, described in the previous section, makes a valid assessment of the affect of the power level on the calculated stability margin very difficult. In order to be realistic in the comparison the axial power profile should be changed, but it is also necessary to maintain approximately the same relation between the initial position of the boiling boundary and the center of the volume in which it occurs.

It was not possible to meet both of these requirements without having an extremely bottom heavy power profile. It was possible, however, to get a general idea of the stability trend as the power increases by ignoring the axial power profile and satisfying only the boiling boundary constraint. Figure #28 shows the power transients for two cases with similar initial boiling boundary positions, one at 58.45% power and the other at 100% power. A reduction in stability with increase in power is indicated.

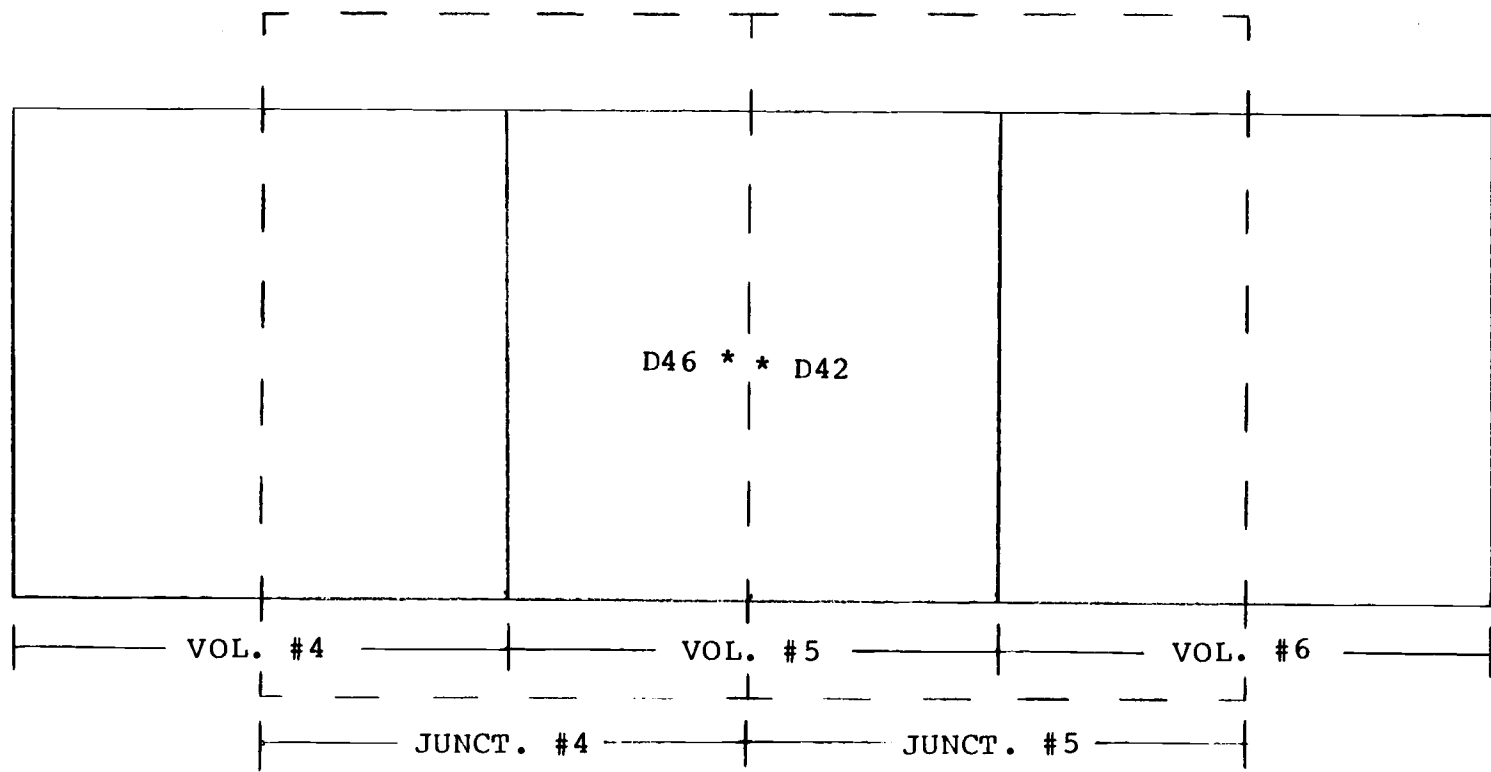


Figure 24. RETRAN control volume/junction geometry.

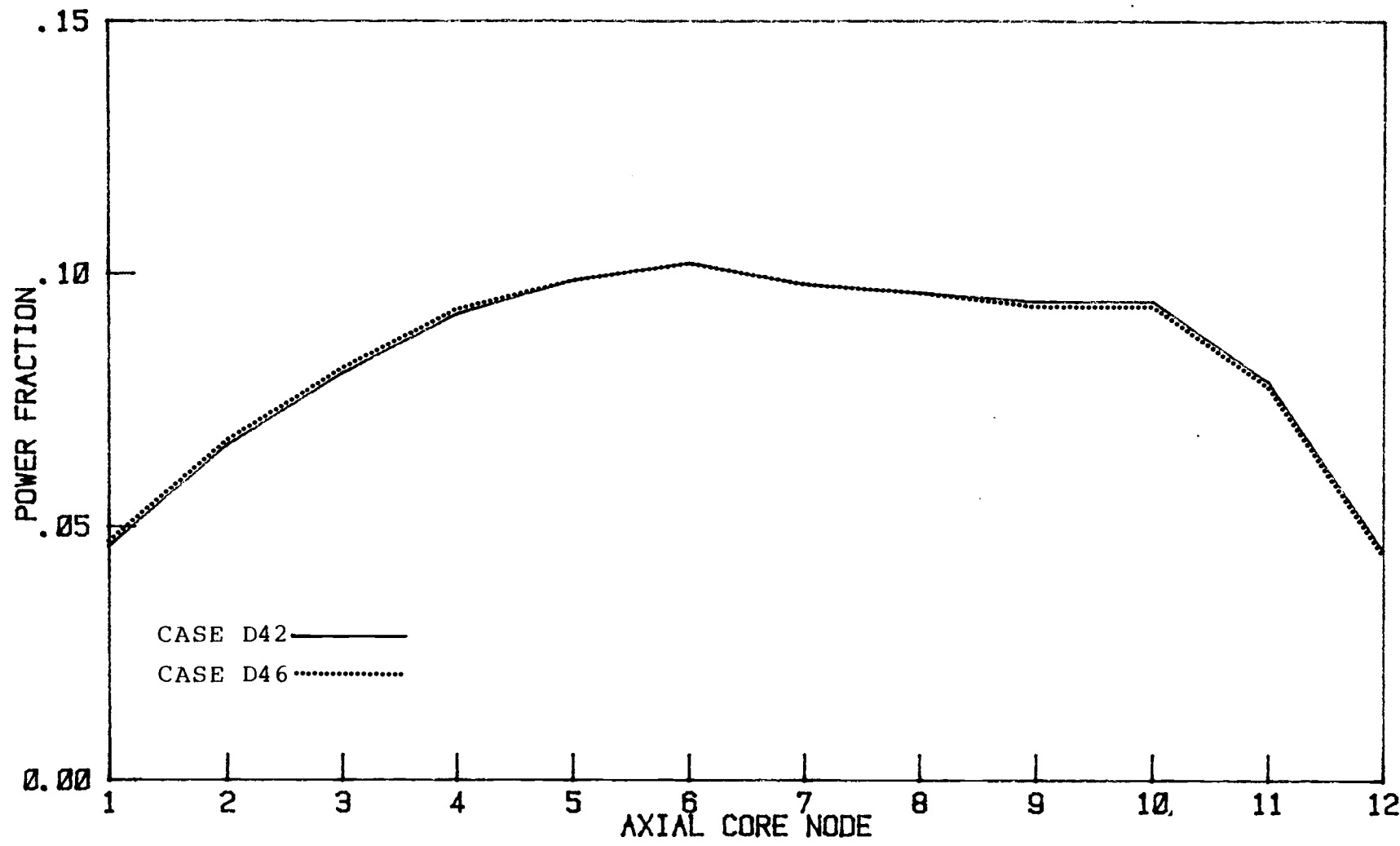


Figure 25. Various axial power profiles used for 100% power cases.

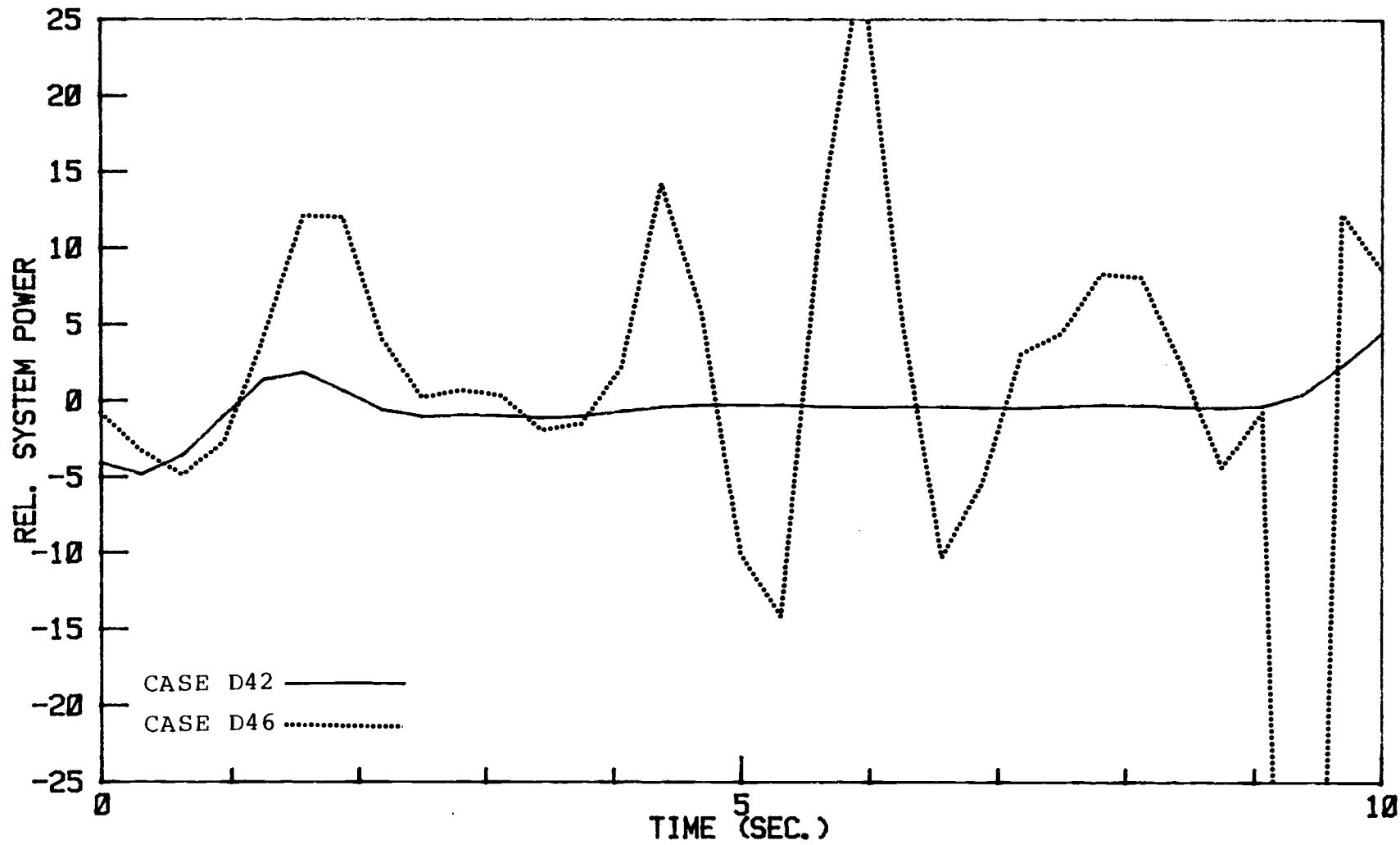


Figure 26. Reactor power transients resulting from extreme cases of the "nodal" effect (ASM for two-phase-flow).

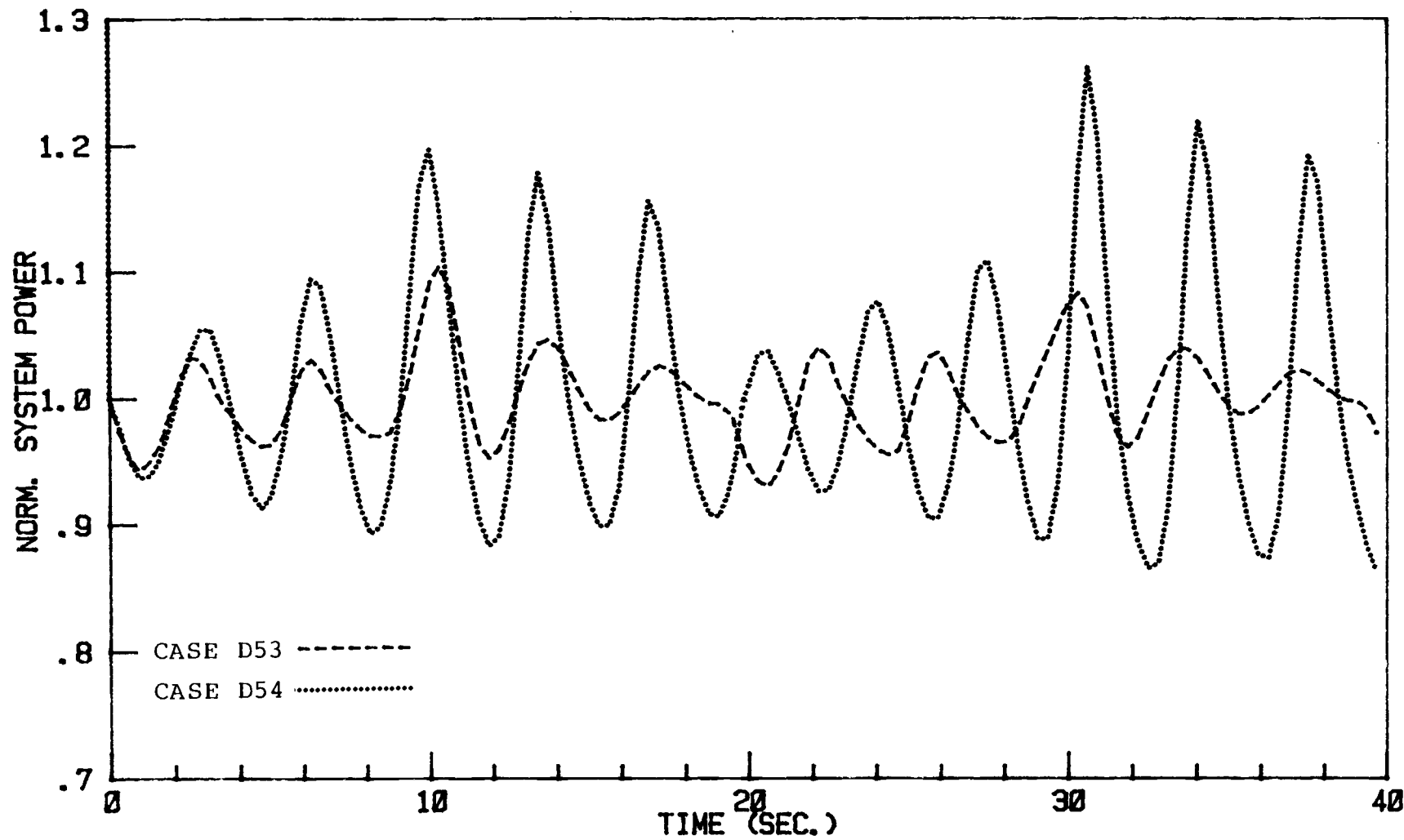


Figure 27. Reactor power transients resulting from extreme cases of the "nodal" effect (HEM for two-phase-flow).

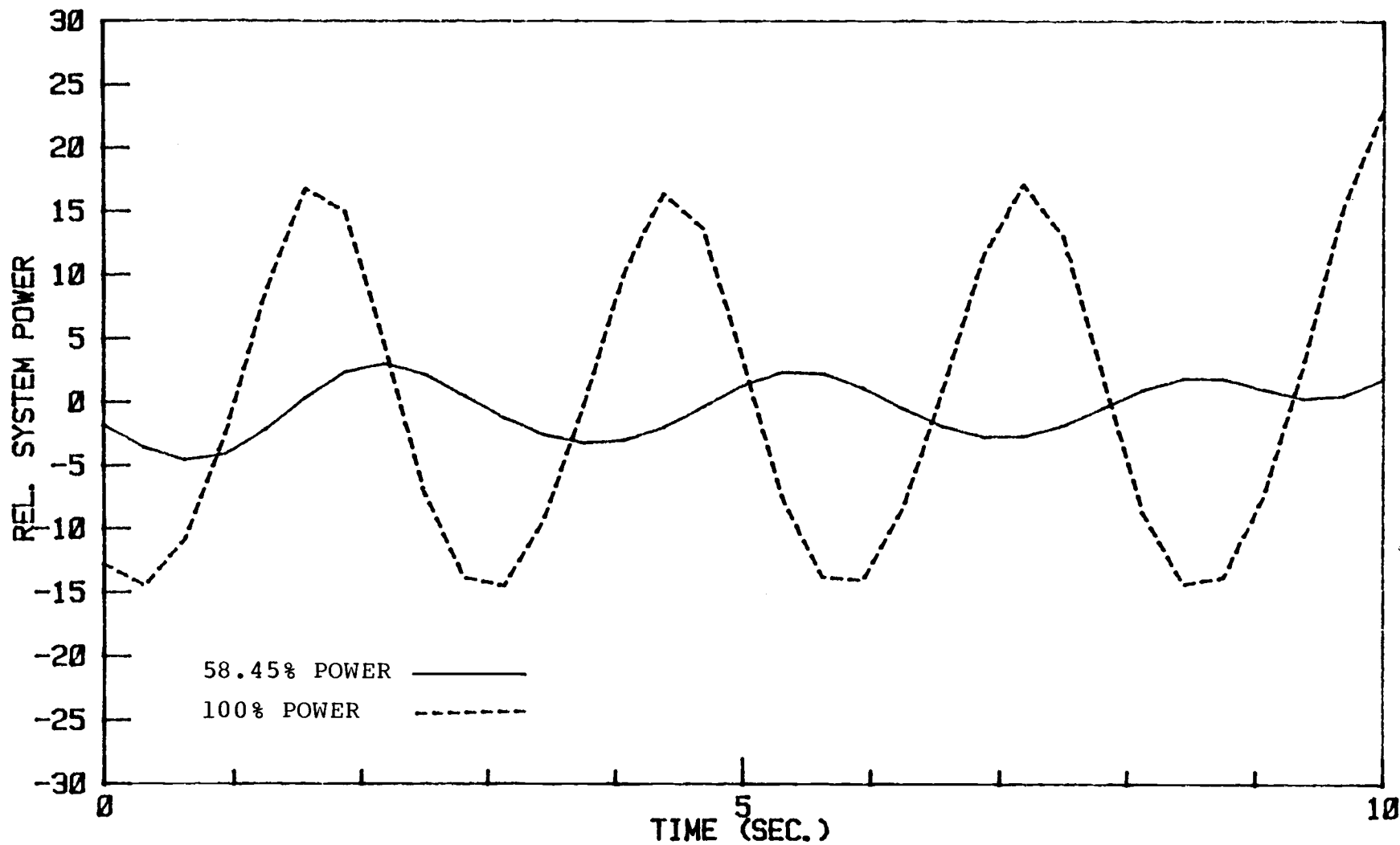


Figure 28. Reactor power transients for 58.45% and 100% initial power.

#### IV. CONCLUSIONS

The simplified version of the RETRAN BWR model used to simulate the PB2 stability tests produces calculated transient results which are essentially equivalent to those produced by the comprehensive model. The use of the time dependent volume offers a valid method for introducing the perturbation signal into the system, but constraints regarding the magnitude of the signal and its representation in the code must be observed. When these constraints are observed the assumption that the model is linear is valid when performing the frequency domain analysis.

The results of the sensitivity studies performed for several modeling options and systems parameters under natural circulation cooling conditions are as follows:

Jet pump modeling technique: The results are insensitive to small changes (10%) in the junction flow area used to model the jet pump suction flow area.

Homologous pump head curves: The homologous pump head curves affect the calculated transient results through their role in determining the total core flow. However, under natural circulation conditions, relatively large

changes in the important parts of the curves produce relatively small changes in the results.

**Two-phase-flow models:** Transient calculations performed using the homogeneous equilibrium mixture model show less stability than cases run under equivalent conditions employing the algebraic slip model. The decrease in stability is a result of the greater change in void fraction per change in power which occurs when the HEM is used.

**Reactor power level:** The RETRAN BWR model calculations show a reduction in stability as the reactor power level increases. This trend is consistent with the observed behavior of operating BWRS.

**Axial power profile:** The results of the axial power profile sensitivity study were inconclusive because of the manner in which the RETRAN code handles the volume in which the boiling boundary occurs. The artificial "nodal effect" is a serious shortcoming in the RETRAN code which should be resolved before the code can be applied to perform reliable stability analyses based on the techniques employed in this thesis.

## V. REFERENCES

1. R.T. Lahey, Jr. and F.J. Moody. "The Thermal-Hydraulics of a Boiling Water Nuclear Reactor". La Grange Park, A.N.S. Publication, 1977.
2. L.A. Carmichael and R.O. Niemi. "Transient and Stability Tests at Peach Bottom Atomic Power Station Unit 2 at End of Cycle 2". EPRI Report NP-564, Palo Alto, June 1978.
3. K. Hornyik and J.A. Naser. "RETRAN Analysis of the Turbin Trip Tests at Peach Bottom Atomic Power Station Unit 2 at End of Cycle 2". EPRI Report NP-1076-SR, Palo Alto, April 1979.
4. BWR Power Plant Training, Nuclear Engineers Manual. General Electric, GEI-92823A, February 1972.
5. T.W. Kerlin. "Frequency Response Testing in Nuclear Reactors". Academic Press, New York, 1974
6. Hewlett-Packard. HP-85 Waveform Analysis Pack. Part No. 00085-90156, Hewlett-Packard, Corvallis, Or. 1980.
7. "RETRAN-02-A Program for Transient Thermal-Hydraulic Analysis of Complex Fluid Flow Systems, Volume 3: Users Manual". EPRI Report NP-1850, Palo Alto, May 1981.
8. "RETRAN-02-A Program for Transient Thermal-Hydraulic Analysis of Complex Fluid Flow Systems, Volume 1: Equations and Numerics". EPRI Report NP-1850, Palo Alto, May 1981.
9. J.E. Hench, G.J. Walke. "Study of Small Breaks and Natural Circulation in BWRs". EPRI Report NP-1564, Palo Alto, October 1980.
10. K. Hornyik. "Special RETRAN Modeling Studies Performed in Conjunction With the Peach Bottom-2 Transient Test Analysis". EPRI Report NP-1842, Palo Alto, May 1981.

11. N.S. Burrell, W.G. Choe, et. al.. "A RELAP4 Analysis of the G.E. BWR Blowdown Heat Transfer Two-Loop Test Apparatus Experiments, Test 4902, 4903, 4904, and 4906". EPRI Report NP-169, Palo Alto, November 1976.
12. S. Forkner, Tennessee Valley Authority, private communication, 1982.
13. David L. Hetrick. "Dynamics of Nuclear Reactors". The University of Chicago Press, Chicago. 1971.
14. K. Hornyik. "RETRAN Analysis of the Stability of BWRs Operating With High Power/Flow Ratio". Final Report, EPRI Research Project 695, July 1982.

## **Appendix**

## VI. APPENDIX

### Frequency Domain Analysis

#### Fourier Transforms

Any periodic time function may be expressed by its Fourier Series, an infinite sum of weighted sine and cosine functions of the fundamental frequency and its harmonics. The Fourier Series may be interpreted as an explicit statement of the frequency content of a periodic time function. The mathematical formulation is:

$$x(t) = \frac{a_0}{2} + \sum_{n=1}^{n=\infty} (a_n \cdot \cos(2\pi nt/T) + b_n \cdot \sin(2\pi nt/T)) \quad (A1)$$

where  $x(t)$  is the periodic time function and  $T$  is the period.

The restriction that the time function be periodic may be removed if it is assumed that the period approaches infinity. In this case the Fourier Expansion is replaced by the Fourier Transform defined by:

$$S_x(f) = \int_{-\infty}^{+\infty} x(t) \exp(-i2\Delta ft) dt \quad (A2)$$

Equation (A2) is in a form for calculation of the transform of a continuous time function. For discrete data points obtained by sampling a time function  $N$  times at intervals  $\Delta t$  the "Discrete Fourier Transform" (DFT), equation (A3), is used.

$$S''_x(m\Delta f) = \Delta t \sum_{n=0}^{N-1} x(n\Delta t) e^{-i2\pi m \Delta f n \Delta t} \quad \text{for } m=0, \dots, N/2 \quad (\text{A3})$$

The discrete Fourier transform differs from the Fourier transform in that frequency information is available in the former only at discrete frequencies,  $f_n$ , and is valid only up to some maximum frequency,  $F_{\max}$ . This upper limit on the frequency may be determined from the relation:

$$F_{\max} = 1/(2\Delta t) \quad (\text{A4})$$

where  $\Delta t$  is the constant sampling interval of the time function. The lower limit of the frequency scale is determined by the time interval over which data points are available, given by  $T = N \cdot \Delta t$ , where  $N$  is the number of data points, thus:

$$F_{\min} = 1/T = 1/(N\Delta t) = \left(2/N\right) \cdot F_{\max} \quad (\text{A5})$$

Calculation of the DFT of a time function,  $x(t)$ , represented discretely by  $N$  data points will produce  $N/2$

complex quantities,  $S''_x(f_n)$ , which contain gain (G) and phase (P) information for the signal content at each of the frequencies  $f_n$ . The gain and phase are determined from the real ( $R_s$ ) and imaginary ( $I_s$ ) parts of the complex quantities,  $S''$ , by the relations:

$$G = \sqrt{R_s^2 + I_s^2} \quad (A6-A)$$

$$P = \text{Arctan}(I_s/R_s) \quad (A6-B)$$

### Transfer Functions

The transfer function of a system can be determined by using the DFTs of an input function,  $x(t)$ , and the corresponding output function,  $y(t)$ , in conjunction with Power Spectrum analysis techniques. The Auto-Power Spectrum and the Cross-Power Spectrum are given, respectively, by the relations:

$$G_{xx}(f) = S_x(f) \cdot S_x^*(f) \quad (A7-A)$$

$$G_{yx}(f) = S_y(f) \cdot S_x^*(f) \quad (A7-B)$$

where the \* superscript indicates the complex conjugate. The transfer function of the system is determined from

these two functions by the relation:

$$H(f) = G_{yx}(f)/G_{xx}(f) \quad (A8)$$

The gain and phase shift of this transfer function for each frequency are given by:

$$G_h(f) = \sqrt{R_h^2 + I_h^2} \quad (A9-A)$$

$$\phi_h = \text{Arctan}(I_h/R_h) \quad (A9-B)$$

### Decay Ratio

At the present time the Decay Ratio (DR) is used to characterize the stability margin of BWRs. The decay ratio describes the dominant underdamped response of the system to a perturbation. The character of the decay ratio is most clearly demonstrated with the application of a Dirac pulse perturbation to a second order system. In this case the decay ratio is a constant, defined as the ratio of successive maxima or minima of the response function, or:

$$DR = y_{i+1}/y_i \quad (A10)$$

The method used to determine the decay ratio for a

transient calculation performed with the RETRAN model is as follows. The calculated transfer function is fitted with a second order transfer function of the form:

$$F(s) = \frac{a(s/w_o) + c}{(s/w_o)^2 + 2d(s/w_o) + 1} \quad (A11)$$

over the frequency range of 0.15 to 0.65 Hz. This range of frequencies normally contains the resonance peak of the transfer function of interest. The parameters  $a$ ,  $c$ ,  $d$ , and  $w_o$  are found by using a non-linear fitting procedure<sup>14</sup>. The relation for the decay ratio can be derived from this fitted second order transfer function as follows. The fitted transfer function, equation (A11), is defined as the ratio of the transforms of the output function,  $\bar{Y}$ , and input function,  $\bar{X}$ . or:

$$F(s) = \bar{Y}/\bar{X} \quad (A12)$$

If the input function is a Dirac delta function,  $\delta(t)$ , the transform,  $\bar{X}$ , is just unity and the transfer function becomes:

$$F(s) = \bar{Y} \quad (A13)$$

The inverse transform is then just the response function, which in this case has the form:

$$y = A \exp(-w_0 \cdot d \cdot t) \sin(w_1 \cdot t + \phi) \quad (\text{Al } 4)$$

were  $w_1 = w_0 \sqrt{1-d^2}$  is the damped resonant frequency. Equations (A10) and (A14) can be combined, with the cycle length equal to the damped resonant frequency, and the following relation for the decay ratio will result:

$$\text{DR} = \exp(-2\pi d / \sqrt{1-d^2}) \quad (\text{Al } 5)$$